ADDIS ABABA UNIVERSITY

ADDIS ABABA INSTITUTE OF TECHNOLOGY

SCHOOL OF GRADUATE STUDIES

ENERGY CENTER

FEASIBILITY STUDY OF OFF-GRID HYBRID SYSTEMS: MINI-HYDRO, PV AND WIND FOR RURAL ELECTRIFICATION IN ETHIOPIA

(STUDY AREA: MOJANA WODERA DISTRICT, NORTH SHEWA, AMHARA REGINAL STATE, ETHIOPIA)

BY

ABRAHAM TESFA

A RESEARCH PAPER SUBMITTED TO ADDIS ABABA INSTITUTE OF TECHNOLOGY, SCHOOL OF GRADUATE STUDIES, ADDIS ABABA UNIVERSITY, FOR PARTIAL FULFILLMENT OF THE REQUIREMENTS FOR MASTERS OF SCIENCE IN ENERGY TECHNOLOGY.

Feasibility Study of Off-Grid Hybrid Systems: Mini-Hydro, PV, and Wind Power Systems for Rural Electrification in Ethiopia

(Study Area: Mojana Wodera District, North Shewa, Amhara Regional State, Ethiopia)

By

Abraham Tesfa

Advisor:

Dr. Getachew Bekele

March 2015

Declaration

I, the undersigned, declare that this thesis is my original work, has not been presented for a degree in this or other university and that all sources of materials used for this have been acknowledged.

Name: Abraham Tesfa

Signature _____

Name of Institution: Addis Ababa University

Date of submission: March 09, 2015.

This thesis has been submitted for examination with my approval as university advisor.

Name of advisors	Signature
Dr. Getachew Bekele	_____

Abstract

Ethiopia is a country of about 85 million people. About 85%of its people are living in rural remote areas. Those rural areas are either inaccessible to the central grid system or not covered by grid extension to date. About 2% of these areas are accessible to electricity. Among those areas is Mojana Wedera District in Amhara Regional State; North Shoa zone. The study area in this district is called Asofe and Filagenet villages. The run-off river Ajana (Mugil Wahsha), which is the focus of this feasibility study, runs through these villages. The study site's location is 9°53'17.62"N and 30° 34'11.41"E. The people in these villages live both is highland and semi lowland with the attitude ranging from 2,860 to 2,400m. Ajana River is a tributary of Jema river and Jema is in turn one of the main water feeders to Blue Nile.

In Asofe and Filagenet, about 4,434 people live. The two villages have 739 households, two 1st to 8th grade schools having about 1000 students with 20 teachers in each school, five flour mills (assumed), two milk processors (assumed), two health posts and five churches. Though this area is rich in economically harnessable renewable energy sources, the people are not benefited from these resources. Among those resources which are not yet exploited are: Small-hydro, Wind and Solar. Without electricity, modern life is unthinkable to these societies.

This feasibility study focuses on hybrid off-grid renewable potentials of Small-Hydropower, Wind and Solar Photovoltaic (PV) with battery backup and Diesel generator to supply the community with continuous electricity for twenty four hours.

HOMER software is used for simulation, optimization and sensitivity analysis of the hybrid system. Given all the necessary inputs to the software, the results showed a list of feasible hybrid electric supply systems sorted out in accordance to their total present cost (NPC) in ascending order. Cost of energy (COE in $/kW), penetration level into the renewable resources (renewable fraction), the amount of Diesel oil used by the generator per year and the generator's working hour per year are also shown in the result list.

In addition, a sensibility analysis is carried out for the major sensitivity components of the hybrid system. The major sensitivity components of the system recognized are the changing price of solar panel and wind turbine against increasing Diesel oil price. From the sensitivity result, solar

energy is not promising in the study area. But, wind turbine is the most promising resource and can easily be utilized. Using the same software, the optimal costs of the hybrid system result is compared with the cost of grid extension to these villages are computed.

The electricity, produced from this hybrid system will replace the conventional energy sources like wood, animal dung and kerosene. Besides, it brings work and technology opportunities linked to the electrical availability which transforms peoples' life style and gives its contribution to the development of the country.

Keywords: Small Hydropower Potential; Wind Energy Potential; Solar Energy Potential; Hybrid; Primary Load; Deferrable Load; Un-gauged Run-Off River, Net Present Cost(NPC).

Acknowledgements

My deepest heartfelt gratitude goes to my advisor Dr. Getachew Bekele for continuously discharging his knowledge and guidance in the time of series of discussions while I was working on the thesis. Without his help, I would not have completed the theses work.

My sincere gratitude and appreciation goes also to Dr.-Ing. Abebayhu Assefa, Head of Energy Center. I remember him reading my mind in times of my problems with some of the subjects, and helped me a lot to go back to the right track and to cop up with my classmates.

I would like to thank Ethiopian Meteorological Agency for their sincere cooperation in issuing me the wind data.

I do not forget the help and assistances I got from the Mojana Wodera District's management and people. I thank them all for their measureable support.

My gratitude also goes to my class mates Yohannes Tesfaye and Haymanot Baynesagn for sharing their experience in the preparation and giving guideline for the better output of this thesis.

I dedicate my thesis to my father Aba Tesfa Ayele, who did not leave me in my birth place in the dark where there is no civilization. Aba, my childhood mentor, though you are not familiar to modern education, you did what is best for me. I know how it is difficult to raise a child of a deceased mother.

I would like to extend my deepest heartfelt gratitude to my wife, W/o Desta Teshome, for her support in my education from high school to my second degree. And for living with me in times of sorrow and joy for the last thirty-four years and for giving me four beautiful children. I know she has carried me all the way with my weaknesses.

Table of Contents

List of Figures

List of Tables

Acronyms

COE	Costs of Energy
CO_2	Carbon dioxide
EEPCo.	Ethiopian Electric Power Corporation
f_{PV}	PV derating factor [%]
GT	Solar radiation incident on the PV array in the current time step [kW/m^2]
$\bar{G}_{T,STC}$	Incident radiation at standard test conditions [1kW/m^2]
G_T	Solar radiation striking the PV array [kW/m^2]
G_T	Coefficient of heat transfer to the surroundings [kW/m$^{2o}{}_C$]
GHG	Greenhouse gas
GIS	Geographical Information Systems
HOMER	**H**ybrid **O**ptimization **M**odel for **E**lectric **R**enewable
kWh	Kilo Watt hour
NREL	National Renewable Energy Laboratory
NAME	National Metrological Agency of Ethiopia
NASA	National Aeronautics and Space Administration
NMSA	National Meteorological Service Agency
NPC	Net present cost
O&M	Operation and maintenances

PV	Photovoltaic
PDF	Probability density function
SMSE	Surface Meteorology and Solar Energy database
SWERA	Solar and Wind Energy Resource Assessment
$T_{C,STC}$	Cell temperature under standard test conditions [25^0c]
T_c	PV cell temperature [^{o}C]
Ta	Ambient temperature [^{o}C]
TERNA	Technical Expertise of Renewable Energy Applications
Y_{PV}	Rated capacity of the PV array, power output under standard test conditions [kW]

Greek Alphabets

α_p	Temperature coefficient of power [% ^{0}c/]
γ	Azimuth of the surface [^{o}]
δ	Solar declination angle[^{o}]
$\eta_{mp,STC}$	Maximum power point efficiency under standard test conditions [%]
η_C	Electrical conversion efficiency of the PV array [%]
θ_z	Zenith angle[^{o}]
θ	Angle of incidence[^{o}]
ϕ	Latitude[^{o}]
ω	Hour angle[^{o}]

Chapter One

Introduction

1.1 Background

Approximately, one-third of the world's population lives in rural areas without access to electricity either to conventional or renewable energy resources. The most important major priority of a country is 'Energy security', 'Drinking water', 'Climate change' and 'Fighting poverty' [1]. Ethiopian is rich in renewable energy resources: hydro, wind and solar. These most abundant energy resources could be utilized to eradicate poverty and be a pillar for the development of the country's economy, fulfilling its energy security. As it is known, Ethiopia is the water tower of Africa. Big rivers and tributaries are available all over the country. Since the country is located near by the Equator, it gets much of the sun rays all over the year. It has also mountain and off-shore wind potential areas.

Form these renewable energy hybrid sources, electrical energy could be generated in economic and ecological sustainable way. The country has a potential to generate 45,000 MW electrical energy from hydropower. Currently, 2000 MW has been extracted from the hydropower sector [2].

Hydro, Solar and Wind energy technologies offer energy independent and sustainable development by using indigenous renewable energy resources and by creating long-term local jobs and industries. Incremental improvement in existing energy networking will be inadequate to meet this growing energy demand. Due to dwindling reserves and ever-growing concerns over the impact of burring carbon fuels on global climate change, fossil fuel source cannot be easily exploited as in the past.

The cost of bringing utility power via transmission and distribution lines to non-electrified remote villages requires huge investment. This is largely due to small household electrical loads and the fact that many villages are located great distances over difficult terrain from the existing grid. Stand-alone small hydropower, solar and wind energy system can provide cost-effective solution. Modest levels of power for lighting, communication, fans, refrigerators, water pumping and cooking is a must for civilized living style. Unfortunately, traditional fossil fuel energy use has had serious and growing negative environmental impact.

Burning of fossil fuels cause CO_2emissions, this in turn causes global warming, air pollution, and overall global environmental degradation. There are also large environmental costs associated with fossil fuel exploitation-from habitat loss and destruction due to strip mining and oil spills to global warming of the atmosphere largely caused by the combustion by-product of carbon dioxide. In addition to that, fossil fuel reserves are not infinite or renewable. Hence, supply is limited

The advantages of renewable energy resources are many: sustainability (cannot be depleted), ubiquity (found everywhere across the world in contrast to fossil fuels and minerals), and essentially nonpolluting and carbon free. The disadvantages of renewable energy resources are: variability, low density, and generally higher initial cost for conversion hardware. Especially with wind plants, large land requirements and noise.

This feasibility study focuses on hybrid off-grid renewable potentials of small-hydro power, wind, and solar photovoltaic (PV) with battery storage and Diesel generator set to supply twenty four hour electricity to these community. The reason preferring hybrid renewable system to individual system is that combined power system is more reliable and sustainable in terms of supplying electricity for rural electrification [1, 3]. This is due to intermittent climate conditions in the area .In heavy rain season, there is little or no sun, and in draught situation, there is little or no water in the river. Besides, the hybrid system has efficiency range of 15-75%, while PV system has 10 % only [3, 4].This indicates that hybrid system minimizes losses and maximizes the energy and secure availability of sustainable energy to the society.

1.2 Statement of the Problem

The remote rural community in many parts of Ethiopia where the grid is not accessible is without running electricity. The community in this research site is one of them. One of the reasons for not availability of electricity for this community is because of the potentials of the renewable resources in the vicinity is not known. This is due to Research on hybrid off-grid green energy: small hydro, wind, and photovoltaic (PV) is not conducted. This site is rich with the three types of renewable energy resources, the potential of the resources as hybrid power for the use of generating electricity is not known to this date. This is because feasibility study on this site, on these resources is not done before. Hence under this context, conducting feasibility study to this site's hybrid resource is justifiable.

1.3 Objectives of the research

1.3.1 General objective

The main objective is to supply electricity to the needy people and improve their life style. This is realizable by first by conducting feasibility study for small hydro, wind and photovoltaic hybrid renewable energy resources for the community. To discover and quantify the green energy potential available with regarding these resources, this feasibility study will pave the way to generate green gas free and eco-friendly electricity from these resources.

1.3.2 Specific objectives

1. To explore and quantify renewable energy potentials for the selected site;
2. To evaluate the technical and economic performance of small-hydro, PV, and wind hybrid system of the selected site;
3. To estimate the electrical load of the community;
4. To provide appropriate information for the government and its stakeholders.

1.4 Scope of the Thesis

1. The scope is to study resources potential according to the selected conversion technique, optimize solution, sensitivity analysis, and comparing the cost of grid extension to that of the standalone hybrid system.
2. Designing physical parts of components is not the scope of this study.

1.5 Significance of the study

When the outcome of the study is realized, it will contribute to assure sustainable and quality life to the remote rural people in this community. The research paper can be used to other similar rural areas. It can be used as reference material for future studies for students in the area. It does have its own contribution for policy makers: hence, government or NGOs shall easily implement rural electrification programs either in this community or in other similar parts of the country. It motivates the people living in this remote area to push the concerned authorities for an access to electricity.

1.6 Organization of the thesis

This thesis paper includes five chapters and appendices. All are organized as follows: Chapter One Introduction: This chapter reviews the rationale for the study. It includes back ground and problem statement, objective of the research (general, specific), scope of the research, significance of the study. Chapter 2: This chapter is divided into four sub-sections. In the first section, previously conducted relevant literatures are reviewed. In the second section, Basics Mini-Hydropower, and Method of Estimating its Potential for Un-gauged River is explained. In the third sub-section of this chapter under "Wind basics and its potential", basics of wind energy (distribution of wind, energy extraction from wind, mountain wind), wind resource in Ethiopia (wind data in Ethiopia and type of wind specific to project site), wind turbine (components are discussed. In the fourth sub-section of this chapter, Photovoltaic basics and the potential: this sub chapter comprises introduction, PV cells, modules, and arrays, photovoltaic working principles, Photovoltaic array output, the radiation incident on the PV array is discussed.

Chapter 3: is on Load Estimation and Input Data to the Software: In this chapter, criteria for potential site identification, method of data collection, what type of software used for simulation, optimization, and sensitivity data analysis for the feasibility study are discussed. Besides, Modeling Hybrid Renewable Energy Systems, typical standalone hybrid system, resource assessment of each relevant renewable resource used in the hybrid system is explained. It is about Electric load estimation, and optimization of Hydro/Wind/PV hybrid systems using HOMER.

Chapter 4: Result and Discussion: Discusses the result of optimization and sensitivity analysis of the system. Chapter five: Conclusion and Recommendation: summarizes the main findings of the thesis work and recommends for those who wants to use as a base either for further study or as an input for information. Appendixes: describe price indexes, specifications, load time schedules, and project site's community and social institutes' information.

Chapter Two

2.1 Literature Review

Many literature references have been reviewed before and during conducting this thesis to have a clear view and knowledge about the subject matter of what am I doing. Some of them which are highly related to this thesis are discussed in this literature review chapter.

S. Ashok [5], Journal on Science Direct, the study is on "optimization Model for Community Based Hybrid Energy System" and is conducted in rural villages in Western Ghats (Karala), India. The hybrid renewable energy sources in the optimized model were Solar PV/Wind/Micro-Hydro with generator and battery backup. The final optimum result from the study shows that Micro-Hydro-Wind is found to be the optimal combination for the electrification of these remote rural villages.

The methodology used is 2^n -1 combination, where 'n' is the type of renewable energy resources used in the study. Hence, there are seven combinations. A parallel hybrid configuration of these components is used in the approach with battery storage and Diesel generator as backup sources. The criterion for selecting the best hybrid energy system combination is the trade-off between reliability, cost, and minimum use of Diesel generator. As the component sizes and operation are interdependent, different set of component configuration were analyzed in each hybrid combination to get the optimal hybrid system. Numerical iterative algorism is used for unit sizing of hybrid energy system that minimizes the capital cost of 2^n -1 combination of the hybrid renewable energy sources. The final optimum result from the study shows that Micro-Hydro-Wind is found to be the optimal combination for the electrification of these remote rural villages.

According to Ashok, the principal demand of electricity for the village is lighting and radio. Hence, he specified 11, and 20W compact fluorescent lamps, and 60W fan, and 35W radio. The unit cost of electricity for the above hybrid system is 0.104 USD.

The methodology used in the analysis to get the final optimum result is similar to the HOMER data analyzing approach. But, the study did not consider the operational characteristics of the optimized systems. Such as annual electrical energy production, annual electrical load served, excess electricity, renewable energy fraction, capacity shortage, unmet electric load. The economical comparison: grid extension versus hybrid systems (Investment

costs) electrification cost of grid extension to that of the standalone renewable hybrid system is not compared and decision is not made with this regard.

Deepak KamarLal [1], International Journal on Electrical Engineering and Informatics, 2011; and two others jointly studied on "Optimization of PV/Wind/Micro-Hydro/ Diesel Hybrid Power System" for remote area of Sundargarh district of Orissa state, India using HOMER optimization software. The feasibility result shows that all the renewable energy resources under the study were feasible with generator set and battery backup. In their feasibility study, annual electrical energy production, annual electrical load served, excess electricity, renewable energy fraction, capacity shortage, unmet electric load is analyzed. The economical comparison: grid extension versus hybrid systems (Investment costs) electrification cost of grid extension to that of the standalone renewable hybrid system is compared. But, the conductors did not comment whether grid extension or the standalone system is the preferable solution. Besides, there is no detail how village load is estimated.

From their conclusion, it is understood that, the optimum result COE of the proposed model is on the higher side of the conventional energy resource. But, the study conductors hope that, in the competitive market, if installation cost decreases, and further technological advancement to the design of hybrid models the COE at present calculated value will dramatically decrease.

Bekele [6] 'Conducted a feasibility study of Solar-Wind Based Standalone Hybrid System for Application in Ethiopia', World Renewable Energy Congress, 2011, Sweden. He took a model of 200 families comprising from 1000 to 2000 family members in total. The site location is Debrezeit, about 47km, South of Addis Ababa. The National Renewable Energy Laboratory's (NREL) HOMER software is used in the simulation and analysis of his data.

Bekele considered the community load as follows: Common electric load for rural village of Ethiopia is composed of lighting, TV, radio, and water pumping, for household, primary schools. For health post: limited clinical equipment such as vaccine refrigerators, communication and AM/FM radios, and microscope.

The final result shows that since wind is found a low potential, is not a promising renewable energy in the aforementioned sample site. But, solar supported by Diesel generator with battery backup is a promising one. The best optimum result of the software is with zero renewable fraction, but the second row with 58% of the renewable solar energy contribution,

and with NPC of $235,177, and the regarding total cost of energy (COE $/KWH) is 0.376was taken as the optimum option.

In his conclusion, extracted from the same overall optimization result table, as HOMER offers a list of schemes ranked on the bases of NPC, he preferred to take the most feasible row which contains 58% of the renewable energy contribution, with the acceptable reasoning that a system is considered as a renewable system if the renewable contribution is 27% and or above. Hence, the regarding row with the NPC of $ 235,177 and COE $/KWH 0.376 is as the most feasible, though this COE 0.376 is on the higher side of the conventional energy resource, which is 0.04 $/KWH.

According to Bekele, the optimization results with renewable fraction from 58% to 85% with the NPC level penetration are considered feasible. But, he left the choice to the policy makers to consider either any of the renewable energy from the list or to stick to the Net Present Cost (NPC). As per his suggestion, utilization of the renewable energy comes first.

2.2 Small Hydropower

2.2.1 Principle of Hydropower

Objective of hydropower is to convert the potential energy of mass of water at certain height termed as head to mechanical energy by the turbine at the downstream side of the flowing water. The mechanical energy produced by the turbine shaft change to electrical energy by the generator for end users.

Adequate head and continuous flow are necessary for hydropower generation. For small hydropower potential weir also has to be available near by the river in which power generation has to take place. The power output from the system is proportional to the water flow and head. The small hydropower potential of a stream with available head is

$$P_{hyd,nom} = \frac{\eta_{hyd} \cdot \rho_{water} \cdot g.hnet.\dot{Q}_{design}}{1000w/kw} \quad (2.1)$$

This thesis's research is on small hydropower in Ajana River, North Showa Zone, Amhara Regional State. The study site's location is 9°53'17.62"N and 30° 34'11.41"E.

2.2.2 Classification of hydropower

i. Classification according to installed capacity

There is no agreed standard for this type of classification. According to IRENA, Hydropower, 2012:

1. Small hydro power: from 1MW to 10MW;
2. Mini hydropower: from 100kW to 1MW;
3. Micro hydropower: from 10kW to 100KW

ii. Classification according to head:

1. High head: 100m and above;
2. Medium head: 30-100m;
3. Low head: 2-30 m

iii. Classification can also be defined as:

1. Run- of-river;
2. Powerhouse located at the base of a dam;
3. Integrated on a canal or in a water supply pipe

2.2.3 Run-off-river un-gauged hydropower system

"Run-off River" refers to a mode of operation in which the hydro power plant uses only the water that is available in the natural flow of water. There is no water storage. In this run-of-river hydropower system type, electricity is produced whenever there is flow of stream at a certain height. When the flow of water falls from the designed flow of water, the turbine coupled with generator stops generating electricity.

For high and medium head systems, construction of weir is necessary to divert water to the intake .From the weir the water follows the course of the low slop canal called tail race and then to the for bay for the settlement of sediments. From the fore bay, water goes to the turbine intake either through short penstock or pressure pipe. And then back to the river through the tail race [7]. The whole process is shown in Figure 2.1.

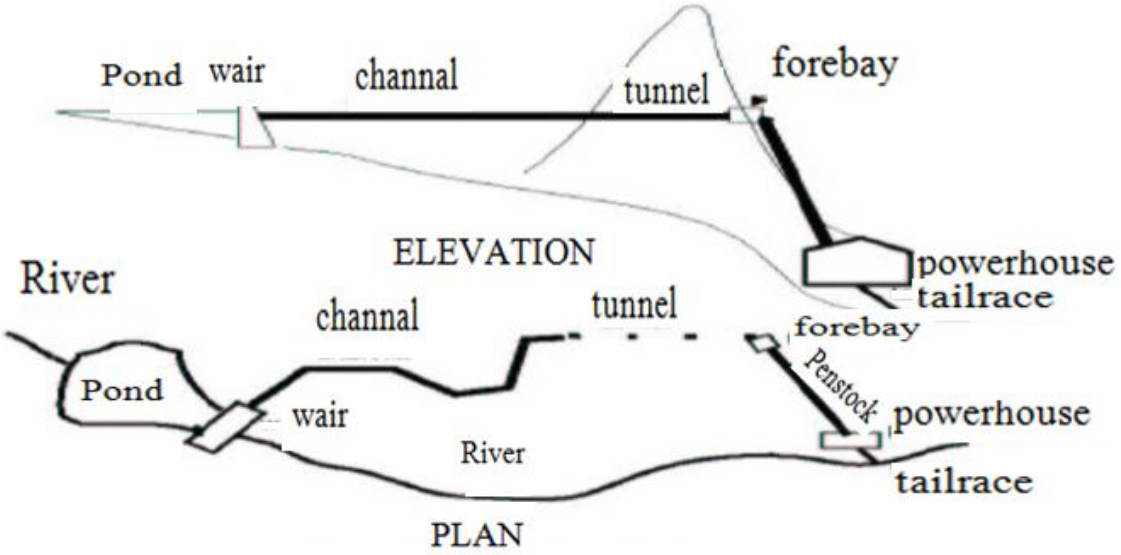

Figure 2.1 Process of high head scheme [7]

i. Gross head

The gross head is the vertical distance that the water falls through in giving up its potential energy (i.e. between the upper and lower water surface levels)

Field measurements of gross head are usually carried out using surveying techniques. GPS tool is used in this project.

ii. Flow/ discharge measurement method for the un-gauged run-off river

For un-gauged river without flow rate data, like the one in this study, manual measurement of flow rate using different methods is a requirement. Among those flow rate measuring methods, velocity area method is used in this thesis [3, 4, 8].The methodology is discussed below.

Velocity–area method

The river under measurement of velocity-area method should have a uniform flow, usually level ground and well defined area at the point of measurement [3, 4].

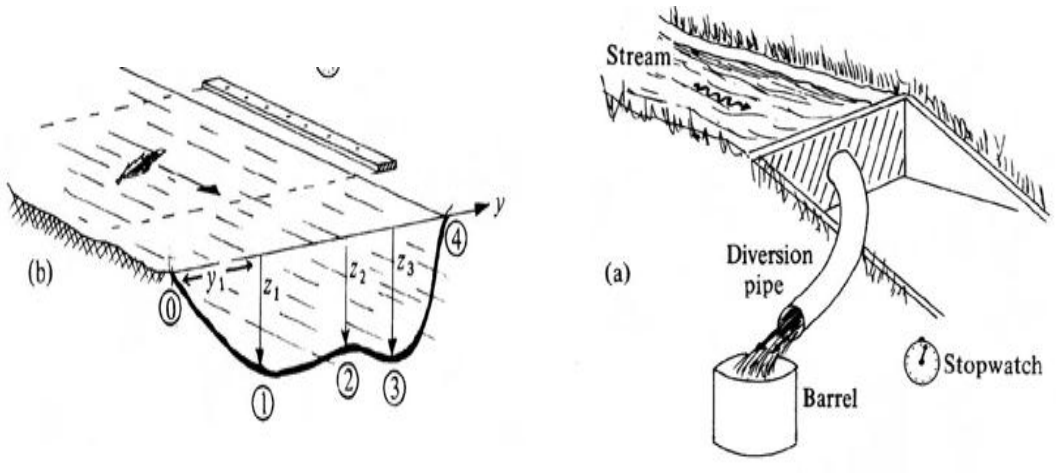

Figure 2.2 Samples of velocity-area measuring methods for un-gauged river [3]

1. Mean velocity measurement

Refined method figure 2.2, defines the mean speed V_{mean} of the flow. Since the flow speed is zero on the bottom of the stream (because of viscous friction), the mean speed will be slightly less than the speed of the float u_s, on the top surface. For a rectangular cross section, it has been found that [10, 11].

$$V_{mean} = 0.8 \times u_s \qquad (2.2)$$

Where u_s, can be measured by simply placing a float, e.g. a leaf, on the surface and measuring the time it takes to go a certain distance along the stream. For best results the measurement should be made where the stream is reasonably straight and uniform cross-section.

2. Measuring the cross-sectional area of the stream

To compute the cross-sectional area of the stream under velocity –area method measurement, the cross- sectional area shall be uniformly divided in to a series of trapezoid [5, 10]. Measuring by marked rules as it is illustrated in figure 2.3.

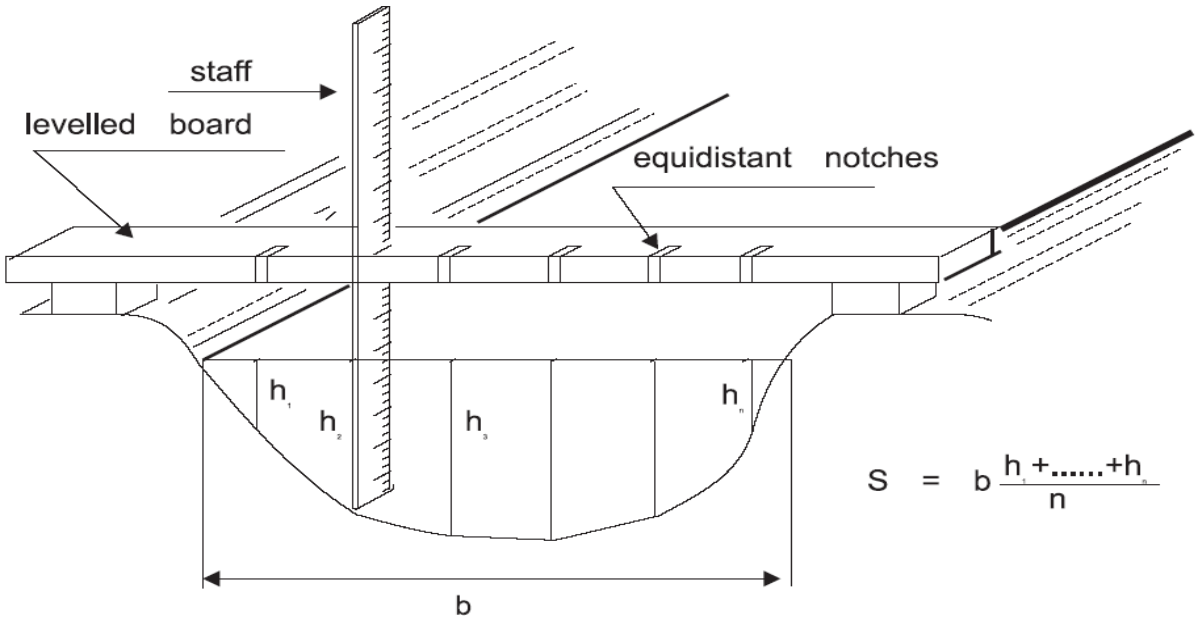

Figure 2.3 Measuring the cross –sectional area [7]

2.2.4 Hydro Turbine

i. Types of hydro turbines

The types of water turbine are mainly classified into two types with some additional classification as follows:

1. Impulse turbine: Pelton turbine
   Cross flow turbine
   Turgo- impels turbine
2. Reaction turbine: Francis turbine
   Propeller turbine

1. Impulse turbine: Turbine type that rotates the runner by the impulse of water jet having the velocity head which has converted from the pressure head at the time of jetting from the nozzle.
2. Reaction turbine: Turbine construction that rotate the runner by the pressure head of flow.

   Shaft arrangement: the arrangement of turbines will be also classified into two types, i.e., “Horizontal shaft (H- shaft)” and “Vertical shaft (V-shaft)”

Referring to the required output, available net head and water low (discharge), the following types of turbine may be applicable for micro or small hydraulic power plant of rural electrification.

1. Horizontal pelton turbine
2. Horizontal Francis turbine
3. Cross flow turbine, Tubular turbine, and Turgo impulse turbine

ii. Hydro turbine selection criteria

Hydro turbine can be selected according to water net head and discharge by using the figure 2.4.

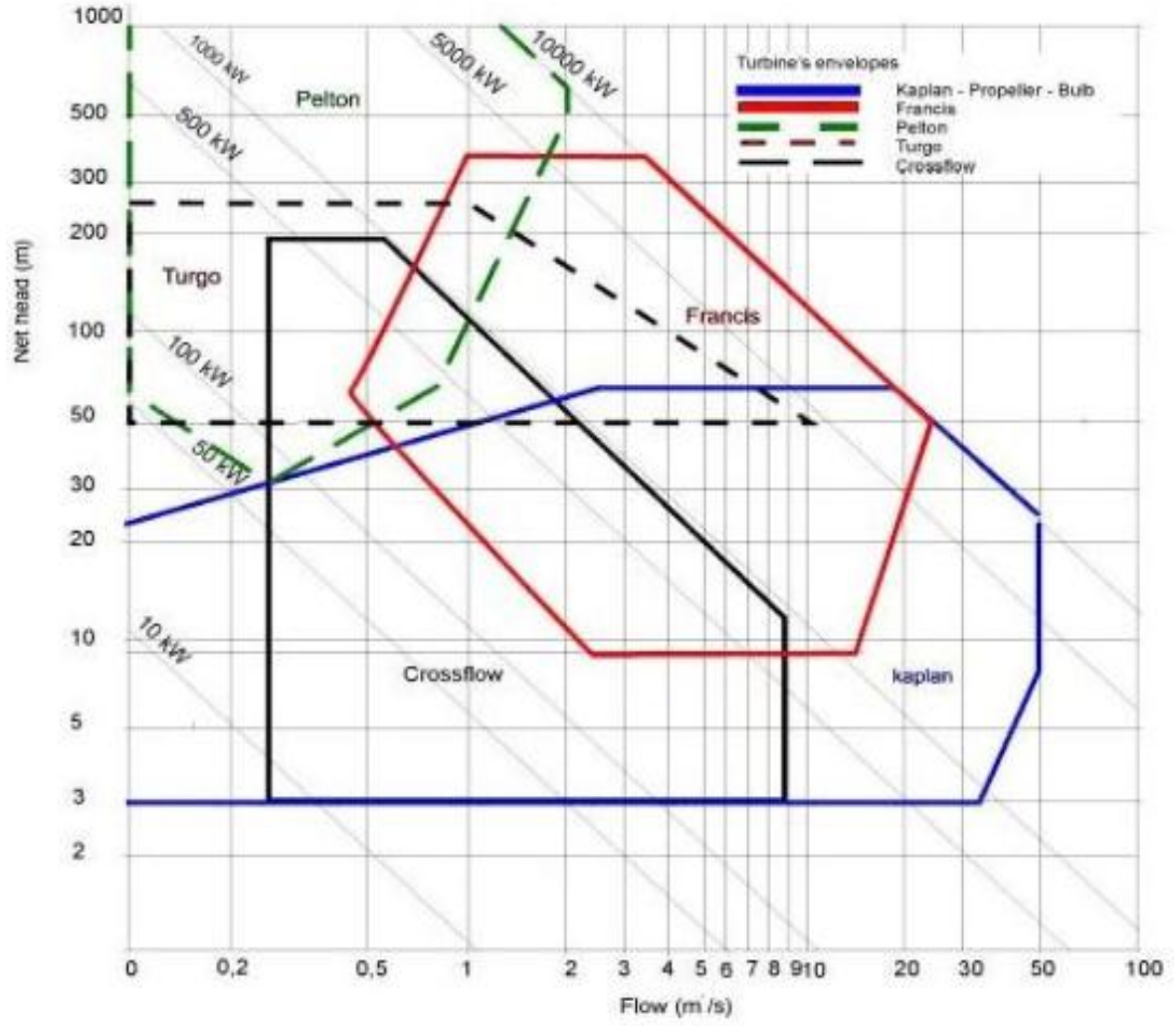

Figure 2.4 Hydro turbine selection chart based on head and flow rate [4, 8, 24]

Since the available head for this project site is 300m, with discharge of 0.053m^3/second, Pelton hydro turbine is selected from this graph of Figure 2.4 for this project site.

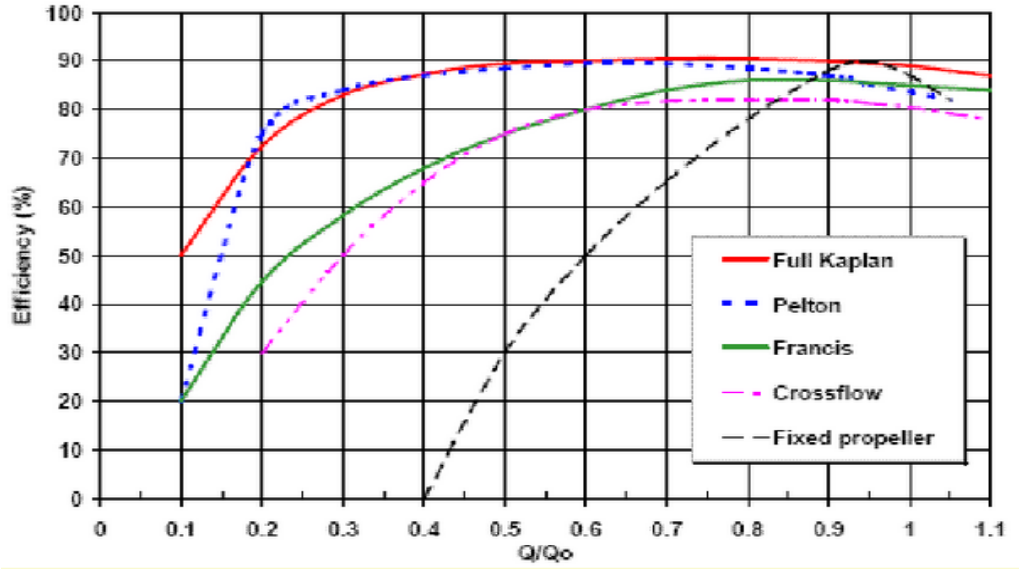

Figure 2.5 Efficiency comparison of different turbines at reduced flow rate [9]

Since the site has a very low flow rate, high in rainy season and low in dry season, Kaplan and Pelton turbine retain their efficiencies with wide flow rate range when running below the design flow Q_O (Figure 2.5), but Kaplan turbine is suitable only for small head(Figure 2.4). Hence, for this high head project case, Pelton turbine is selected.

2.3 Wind Basics and the Potential

2.3.1 Introduction

Wind energy has been used for thousand years for milling grain, sailing ships, pumping water, and other mechanical power application. Today, there are hundred thousand of wind mills in operation around the world many of them are used for water pumping. Now days, the use of wind energy as a pollution free, for generating electricity on a significant scale attracting most current interest in the subject.

Modern windmills tend to be called wind turbines, because of their function similarity to the steam, hydro, and gas turbines that are used to generate electricity. These are used in many countries with wind power potential.

Wind created from expansion and convection of air as solar radiation is absorbed on earth. On a global scale these thermal effects combine with dynamic effects from the Earth's rotation to produce prevailing wind patterns. Besides this general behavior of the atmosphere,

there is local variation due to geographical and environmental factors [10]. One of the results of these factors is the Ethiopia mountain wind in this thesis's site location. This is discussed in depth in the title "Mountain wind".

The wind price is decreasing from time to time. The world's wind turbine price is from 2008 to 2012 is shown in the appendix.

2.3.2 Prevailing wind direction

Prevailing wind directions are important when seating wind turbines. Wind turbines must be seated in the areas with least obstacles from the prevailing wind direction. The rotor of the turbine must be facing against the direction of the prevailing wind direction. In our study site case, the prevailing wind direction is NE.

Table 2.1 Prevailing wind direction regions of the world [11]

Latitude	90-60° N	0-30° N	30-60° N	60-90° N	60-30° N	30-0° N
Direction	NE	SE	NW	SW	SW	NE

2.3.3 Mountain wind

In Ethiopia, mountain wind is created as a result of solar radiation. This happens due to uneven heating and cooling of a particular area. This creates a pressure zone that makers air to flow from high to low pressure areas [11]. Figure 1, is a description for the basic effect of mountain wind. This is the nature of how mountain wind is created in this project site. Topography of the project site is similar to figure 2.6.

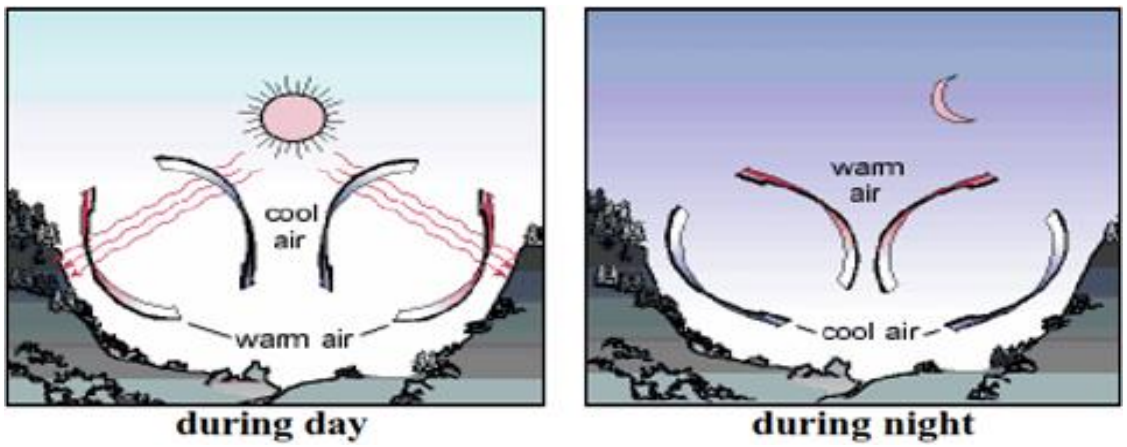

Figure 2.6 Creation of mountain wind in mixed mountain and gorge area [11]

2.3.4 Wind potential in Ethiopia

Studied wind potential areas in Ethiopia are shown in figure 2.7 and figure 2.8[11]. Since project site topography is very similar to Debrebirhan's topography, taking Debrebirhan's data is logical. Hence, project site average wind speed is 5.72 m/s.

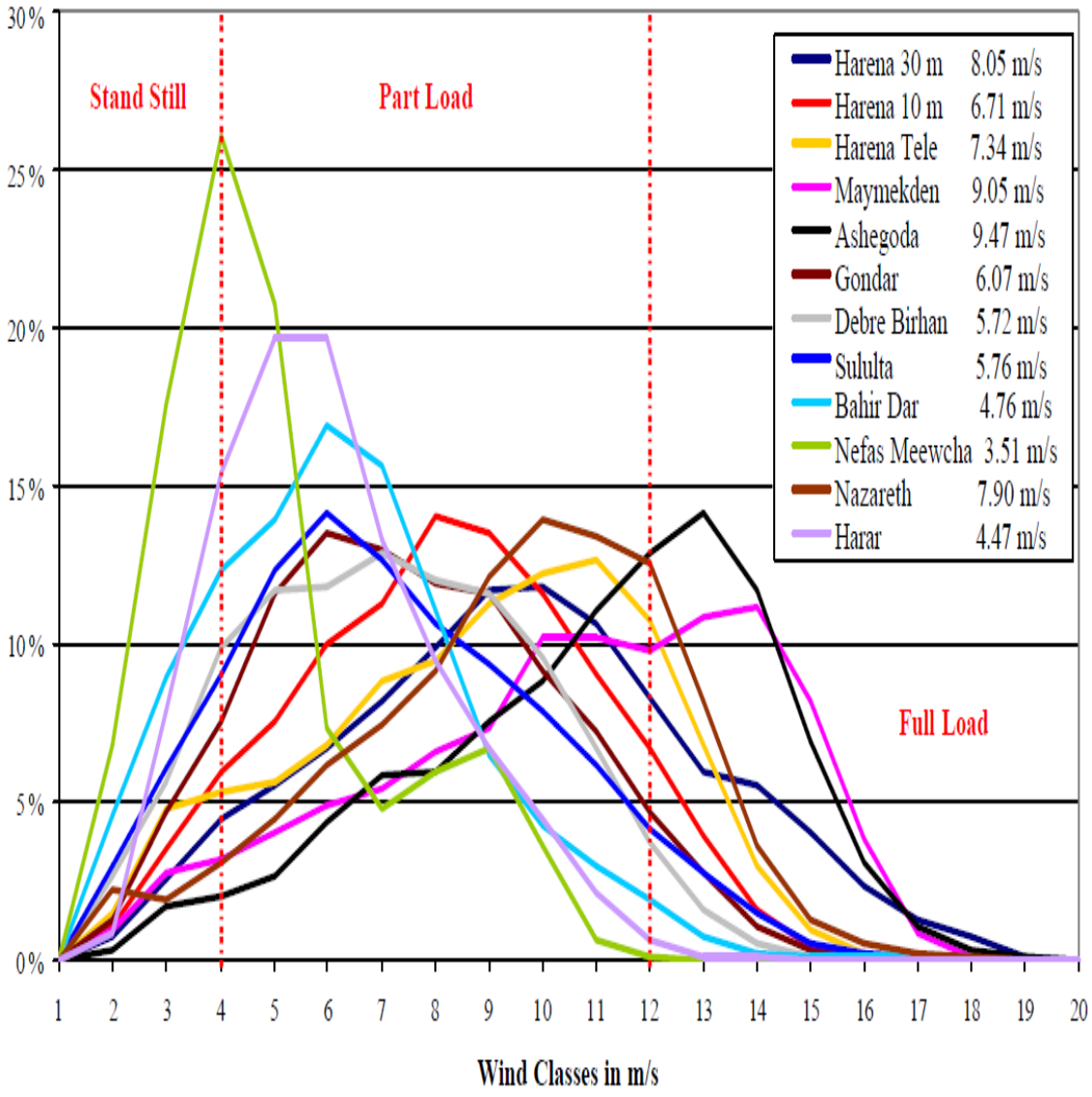

Figure 2.7 Ethiopia's wind potential areas graph [11]

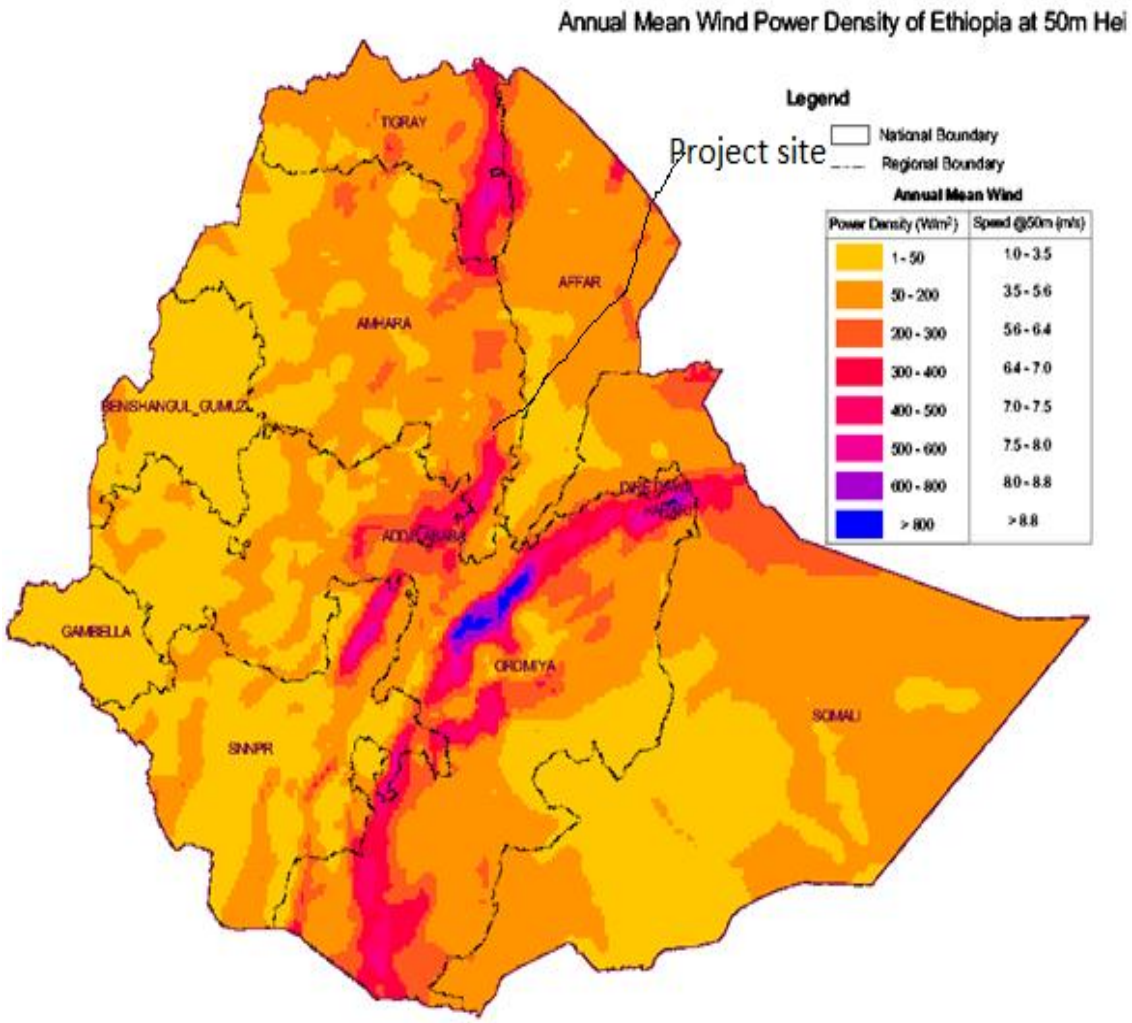

Figure. 2.8 A GIS map showing geographic distribution of wind resources of Ethiopia (Source: SWERA)

The wind resource classifications, Class 1 to Class 7 are indicated by color-codes. Each color code has an assigned range of values to present annual wind power density in W/m^2. Wind resources data are significant for the long term wind power forecasting to establish a reliable hybrid energy system.

Hence, this thesis's conducting site is in the regions of annual average mean wind speed from 5.6 to 6.4 m/s as its annual average is minimum 5m/s.

2.3.5 Power extracted from wind turbines

Power and energy output of wind Turbines the wind turbines converts the force of the wind into torque acting on the rotor blades to generator power. The amount of energy which the wind transfers to the rotor depends on the density of airρ_a , the rotor area A_T, and the wind speed V [10]. The theoretical power extracted from the wind turbine is

$$P_Z = \frac{1}{2}\rho_a A_T V^3 \quad (2.3)$$

And the density of Air is

$$\rho_a = \frac{353-049}{T} e^{-\left(\frac{0.0034z}{T}\right)} \quad (2.4)$$

The air density may be taken as 0.85 Kg/m^{3}for the practical areas.

The rotor swept area A_T determines how much energy a wind turbine able to generator from wind. Since the rotor area increase with the square of the rotor diameter, a turbine which is twice as large will receive four times much energy [10]. In addition the energy on the wind is proportional to the cube of the wind speed.

Extracted power:

$$P_m = \frac{1}{2}m\left(V^2 - {V_o}^2\right) = \frac{1}{2}\rho_a v(V^2 - V_o^2) = \frac{1}{2}\rho_a A_T V * V^2 \left(\frac{v^2 - v_o^2}{V^2}\right) = \frac{1}{2}\rho_a A_T v^3 \left(1 - \frac{v_o^2}{v^2}\right) \quad (2.5)$$

P_m is mechanical power extracted by the rotor, $m\ is$ mass of air per second, and V and V_o are upstream and downstream wind velocity. It is the entrance of the rotor loaded and downstream wind velocity at the exit of the rotor blades respectively [10].

$$P_m = \frac{1}{2}\sigma_a A_T v^3 \left(1 + \frac{v_o}{v}\right)\left(1 - \frac{v_o}{v}\right) \quad (2.6)$$

$$P_m = \frac{1}{2}\rho_a A_T V^3 C_P \quad (2.7)$$

Where $C_P = \left(1 + \frac{V_o}{V}\right)\left(1 - \frac{V_o}{V}\right)$ and it is known as power coefficient of the motor or rotor efficiency. The value of $C_P$depends on the ratio downstream to the upper stream wind speed [10].

In order to provide a reference to this power output, it is compared to the power of the free air stream which flow the same cross-sectional area A_T, without mechanical power being extracted from it.

Betz limit:

Is a theoretical limit on the amount of power that can be extracted by wind turbine from air stream. The limit is

$$C_p = 16/27 = 59\% \quad (2.8)$$

The ideal power coefficient or efficiency graph is shown in figure 2.9.

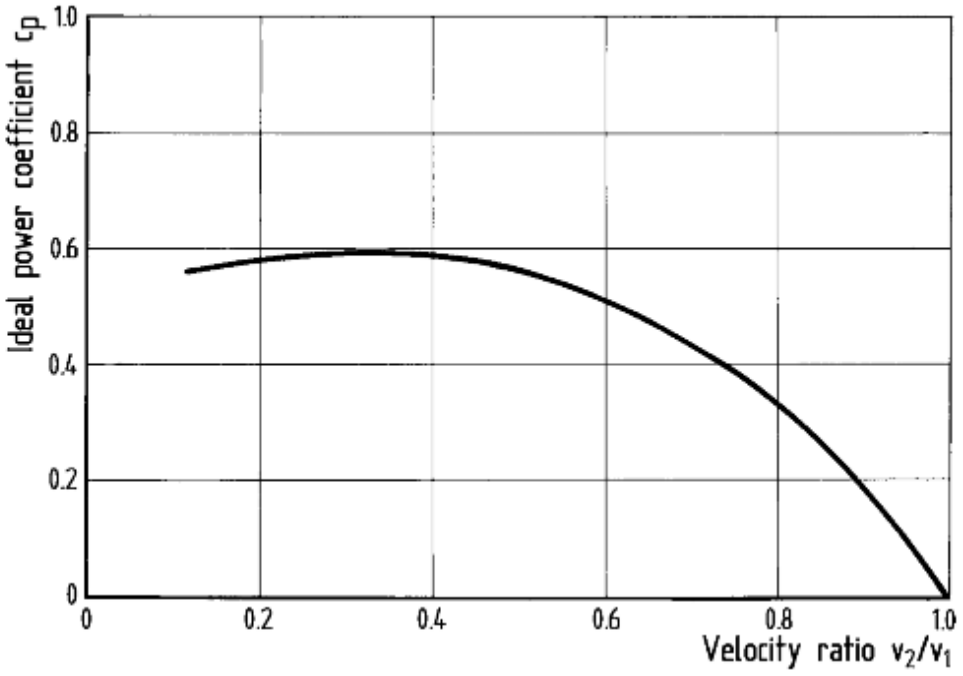

Figure 2.9 Power coefficient versus the flow velocity ratio of the flow before and after the energy converter [10]

2.3.6 Wind turbine power curve

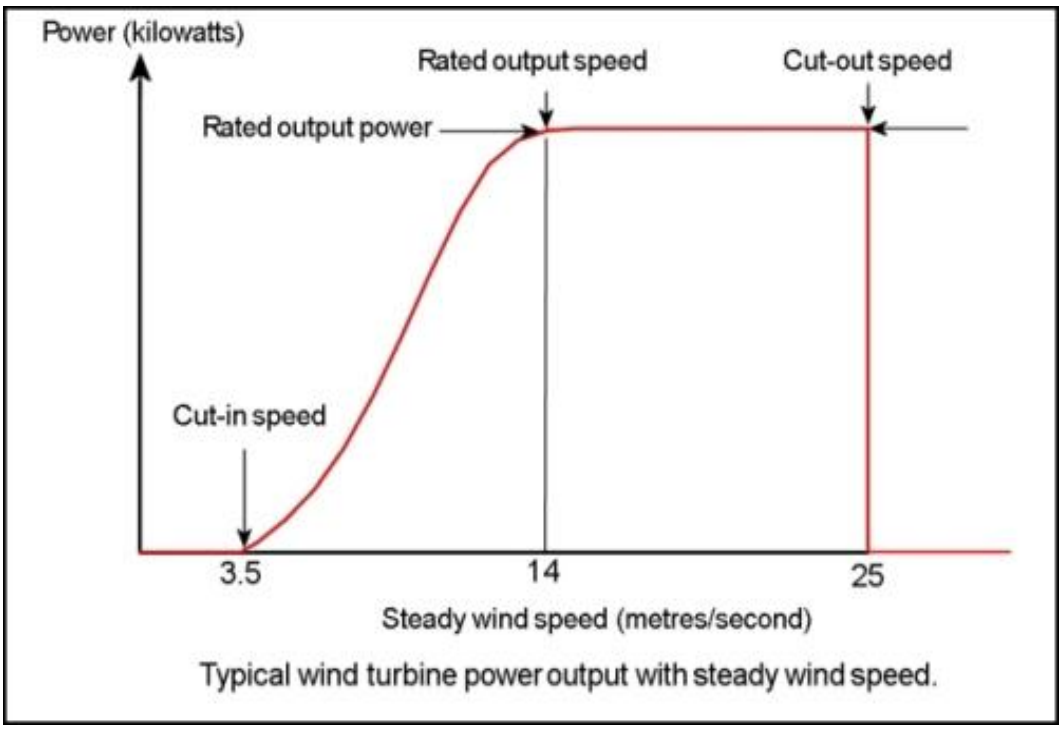

Figure 2.10 Power curve of a typical wind turbine [10]

Cut-in speed: the speed at which the turbine first starts to rotate and generates power, usually between 3 to 4m/sec.

Rated output speed and Rated output power: as the wind speed rises above the cut-in speed, the level of electrical output power rises rapidly to the power that the electrical generator is capable of. This limit to the generator output is called the rated output power and the wind speed at which it is reached is called rated output wind speed.

Cut-out speed: as the speed increases above the rated output wind speed, the forces on the turbine structure continue to rise, and at some point there a risk of damage to the rotor. As a result a braking system is employed to bring the rotor to stand still. This is called a cut-out speed and is usually 25 m/sec.

2.3.7 Analysis of wind data

For estimating the wind energy potential of the site the wind data collected from the location should be properly analyzed and interpreted [13].For wind energy calculations the

velocity should be weighed for its power content while computing the average, hence the average wind velocity may be estimated.

$$V_m = \left[\frac{1}{n}\sum_{i=1}^{n} V_i^{\,3}\right]^{\frac{1}{3}} \quad (2.9)$$

Where V_m is average wind velocity, n is number of wind data

Apart from the average wind velocity over a period its distribution is also acoustical factor in wind resource assessment. The power generated from wind turbines installed at two sites with the same average velocity may be entirely different because of differences in the velocity distribution.

Various probability functions are fitted with the field data to identify suitable statistical distributions for representing wind regimes. It is found that the Weibull and Rayleigh distributions are normally used to describe the wind variations in a region with an acceptable accuracy level.

i. Weibull distribution:

In weibull distribution, the variations in wind velocity are characterized by the two functions;

1) The probability density function and (2) The cumulative distribution function.

The probability density function (f (v)) indicates the fraction of time (or probability) for which the wind is at a given velocity V and is expressed as:

$$f(v) = \frac{k}{c}\left[\frac{v}{c}\right]^{k-1} e^{-(v/c)^k} \quad (2.10)$$

Here, k is the Weibull shape factor and c is scale factor

The cumulative distribution function of the velocity V gives us the fraction of time (or probability) that the wind velocity is equal or lower than V. Thus the cumulative distribution

F (V) is the integral of the probability density function. Thus,

$$F(v) = \int_0^{\infty} f(v)dv = 1 - e^{-(v/c)^k} \quad (2.11)$$

Under the Weibull distribution, the major factor determining the uniformity of wind is the shape factor k and uniformity of wind at a site increases with the shape factor k. For analyzing a wind system following the Weibul distribution, the Weibull parameters k and c must be estimated.

ii. Rayleigh distributions:

For precise calculation of k and c adequate wind data collection short time intervals is essential. When there is no this data, the existing data may be in the form of the mean wind velocity in the form of over a given time period. Under such situation, a simplified model can be derived by estimating k as 2 and simply substitute is the Weibull equations. This is known as Rayleigh distributions [3].

2.3.8 Wind turbine components

Figure 2.11 is the picture of small wind turbine used in this feasibility study.

Figure 2.11 Chinook E17-65 used in the specification of this study [WWW.eoltec.com]

The major components of a commercial wind turbine are

1. Tower
2. Rotor
3. Generator
4. Gearbox or Gearless(Direct drive)
5. Sensors and Yaw drive
6 Power regulation and controlling units

2.3.9 Impact of tower height on wind velocity and power

Wind velocity increases with height due to wind shear. Hence, the taller the tower the higher will be the power available to the rotor Figure 2.12. The available power depends with the rate surface roughness of the ground [6, 12, 13].Hence, the ratio of velocities at two heights Z_r and Z_0 is given by the following equation.

$$\frac{v(Z_{hub})}{v(Z_{anem})} = \frac{\ln(Z_{hub}/Z_o)}{\ln(Z_{anem}/Z_o)} \quad (2.12)$$

Where:

Z_{hub}= the hub height of the wind turbine[m]

Z_{hub}= the anemometer height [m]

Z_0= the surface roughness length [m]

$v(Z_{hub})$= wind speed at the hub height of the wind turbine [m/s]

$v(Z_{anem})$= wind speed at the anemometer height [m/s]

$\ln(Z_{hub}/Z_o)$ = the natural logarithm

The surface roughness length is a parameter that characterizes the roughness of the surrounding terrain. Table 2.2 contains the representative surface roughness length [13].

Table 2.2. Terrain description for surface roughness [13].

Terrain Description	z_0
Very smooth, ice or mud	0.00001 m
Calm open sea	0.0002 m
Blown sea	0.0005 m
Snow surface	0.003 m
Lawn grass	0.008 m
Rough pasture	0.010 m
Fallow field	0.03 m
Crops	0.05 m
Few trees	0.1 m
Many trees, few building	0.25 m
Forest and woodlands	0.5 m

Suburbs	1.5 m
City center, tall building	3.0 m

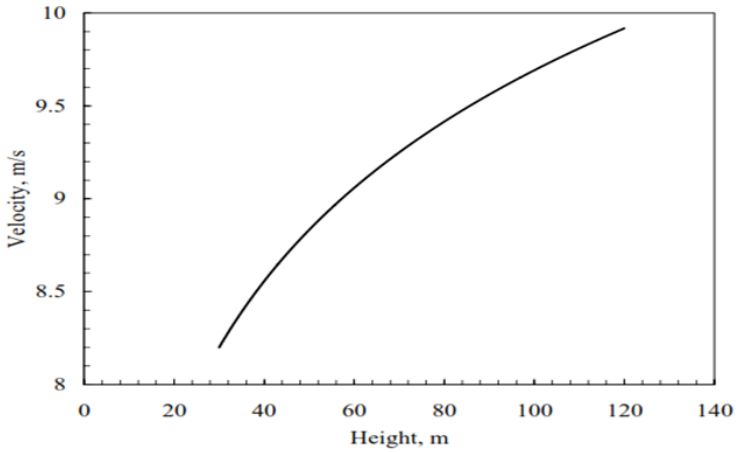

Figure 2.12 Figure Effect of tower height on the velocity at hub height [12].

2.4 Photovoltaic Basics and the Potential

2.4.1 Introduction

Photovoltaic (PV) systems are solar energy systems that produce electricity directly from sunlight using devices called solar cell modules. It is one of the most useful renewable energy systems. All over the world, people are taking up the technology to provide power for many remote and rural applications. A common application of PV technology is providing power for watches and radios. On a large scale many utilities used to provide consumers with solar generated electricity. The photovoltaic cell is made mostly from Silicon, the second most abundant element on the earth's crest.

2.4.2 PV Cells, Module, and Arrays

Photovoltaic cells are connected electrically in series and/or parallel circuits to produce higher voltages, currents and power levels. Photovoltaic modules consist of PV cell circuits sealed in an environmentally protective laminate, and are the fundamental building block of PV systems. Photovoltaic panels include one or more PV modules assembled as a pre-wired, field -installable unit. A Photovoltaic array is the complete power –generating unit, consisting of any number of PV modules and panels.

The performance of PV modules and arrays are generally rated according to their maximum DC power out put (watts) under standared test conditions STC). Standard test conditions are defined by a moduel (cell) operating temperature of 25°C(77°F),and incisent solar irradiance level of 1000 W/m^2 and under Air Mass 1.5 spectral distribution. Since these conditions are not always typical of how PV modules and arrys operate in the field, actual performance is usually 85 to95 percent of the STC rating.

The basic unit of photovoltaic system is the photovoltaic cell. Cells are electrical devices about 1/100^{th} of an inch thick that convert sun light into direct current electricity through the photovoltaic effect. They do not consume fuel and have a life span of about 25 years.

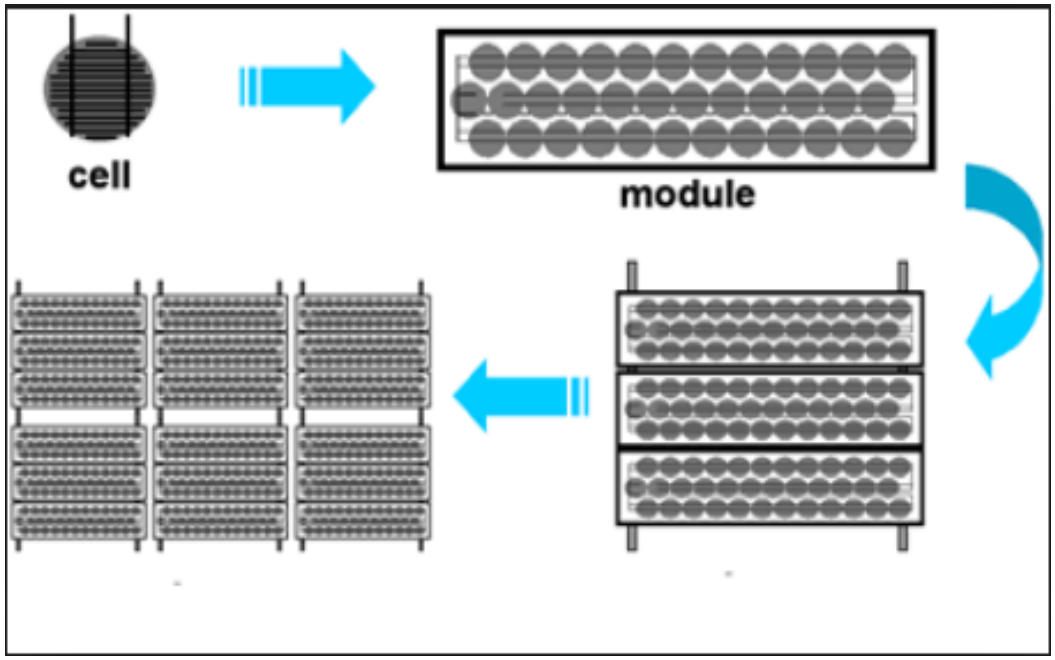

Figure 2.13 Photovoltaic cells, modules, panles and arrays[18].

A module is an assembly of photovoltaic cells wired in series or series/parallel to produce the desired voltage, current, and power. When cells are wired in series, the voltage is additive while the current remains constant. And when cells wired in parallel, current is additive while voltage remains constant.

A module or array can convert about 10 to 15% of the solar energy they receive from the sun to a usable electrical energy. At solar noon on a clear day, an array may receive 1000W of solar radiation per square meter. This would result in approximately 100W of peak power per square meter of array.

2.4.3 Photovoltaic Working Principles

Regardless of size, a typical silicon PV cell produces about 0.5 – 0.6 volt DC under open-circuit, no-load conditions. The current and power output of a PV cell depends on its efficiency and size (surface area), and is proportional to the intensity of sunlight striking the surface of the cell.

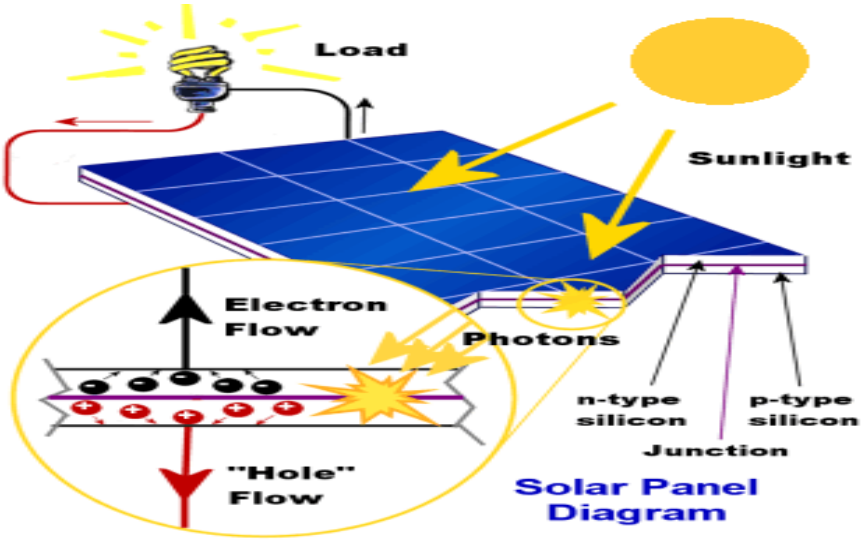

Figure 2.14 Diagram of photovoltaic cell. Florida Solar Energy Center [19]

2.4.4 Output Photovoltaic Array Power

HOMER uses the following equation to calculate the output of the PV array on a tilted surface [20].

$$P_{PV} = Y_{PV} f_{PV} \left(\frac{\bar{G}_T}{\bar{G}_{T,STC}}\right)\left[1 + \alpha_P\left(T_C - T_{C,STC}\right)\right] \quad (2.13)$$

Where:

Y_{PV} is the rated capacity of the PV array, meaning its power output under standard test conditions [kw]

f_{PV} is the pv derating factor [%]

$\bar{G}_T$ is the solar radiation incident on the P array in the current time step [kW/m^2]\

$\bar{G}_{T,STC}$ is the incedent radition at standard test conditions [kW/m^2]

$\alpha_P$is the temperature coefficient of power [% / ^{o}c]

T_C is the PV cell temperature in the current time step [^{o}c]

$T_{C,STC}$ is the PV cell temperature under standard test conditions [25^{o}c]

If on the inputs window you chose not to module the effect of temperature on the PV array, HOMER assumes that the temperature coefficient of power is zero, so that the above equation simplifies to.

$$P_{PV} = Y_{PV} f_{PV} \left(\frac{\bar{G}_T}{\bar{G}_{T,STC}} \right) \quad (2.14)$$

2.4.5 The radiation incident on the PV array

From the PV output equation, one of the parameters, global radiation incident on the tilted PV array could be calculated and found by the following approach [Duffie and Beckman 1991].

We can describe the orientation of the PV array using two parameters, a slope and an azimuth. The slope is the angle formed between the surface of the panel and the horizontal, so a slope of zero indicates a horizontal orientation, whereas a 90° slope indicates a vertical orientation. The azimuth is the direction towards which the surface faces. HOMER uses the convention whereby zero azimuths correspond to due south, and positive values refer to west-facing orientations. So an azimuth of -45° corresponds to a southeast-facing orientation, and an azimuth of 90° corresponds to a west-facing orientation.

The other factors relevant to the geometry of the situation are the latitude, the time of year, and the time of day. The time of year affects the solar declination, which is the latitude at which the sun's rays are perpendicular to the earth's surface at solar noon. HOMER uses the following equation to calculate the solar declination:

$$\delta = 23.45^\circ \sin\left(360^\circ \frac{284+n}{365}\right) \quad (2.15)$$

Where:

n is the day of the year [a number 1 through 365]

The time of day affects the location of the sun in the sky, which we can describe by an hour angle. HOMER uses the convention whereby the hour angle is zero at solar noon (the time of day at which the sun is at its highest point in the sky), negative before solar noon, and positive after solar noon. HOMER uses the following equation to calculate the hour angle:

$$\omega = (t_s - 12hr).\,15^{\circ}/hr \qquad (2.16)$$

Where:

$t_s$is the solar time [hr]

Now, for a surface with any orientation, we can define the angle of incidence, meaning the angle between the sun's beam radiation and the normal to the surface, using the following equation: Calculate solar time from civil time using the following equation:

$$t_s = t_c + \frac{\lambda}{15^{\circ}/hr} - z_c + E \qquad (2.17)$$

where

t_c is the civil time in hours corresponding to the midpoint of the time step [hr]

λ is the longitude [°]

Z_c is the time zone in hours east of GMT [hr]

E is the equation of time [hr]

The equation of time accounts for the effects of obliquity (the tilt of the earth's axis of rotation relative to the plane of the ecliptic) and the eccentricity of the earth's orbit. HOMER calculates the equation of time as follows:

$$E = 3.82[0.000075 + 0.001868.\cos B - 0.032077.\sin B - 0.014615.\cos 2B - 0.04089.Sin2B]$$

2.18)

Where B is given by:

$B = 360^{\circ}\frac{(n-1)}{365}$(2.19)

$\cos\theta =$

$\sin\delta\sin\phi\cos\beta - \sin\delta\cos\phi\sin\beta\cos\gamma + \cos\delta\cos\phi\,cos\beta\cos\omega + \cos\delta\sin\phi\sin\beta\cos\omega +$

$\cos\delta\sin\beta\sin\gamma\sin\omega$ (2.20)

Where : θ is the angle of incidence [^{o}]

β is the slope of the surface[^{o}]

γ is the azimuth of the surface[^{o}]

ϕ is the latitude [^{o}]

δ is the solar declination [^{o}]

ω is the hour angle [^{o}]

An incidence angle of particular importance

Which we will need shortly, is the *zenith angle*, meaning the angle between a vertical line and the line to the sun. The zenith angle is zero when the sun is directly overhead and 90° when the sun is at the horizon. Because a horizontal surface has a slope of zero, we can find a equation for the zenith angle by setting β = 0° in the above equation, which yields:

$\cos\theta_z = \cos\phi\cos\delta\ \cos\omega + \sin\phi\sin\delta$(2.21)

Where:

θ_z is the zenith angle[°]

Now we turn to the issue of the amount of solar radiation arriving at the top of the atmosphere over a particular point on the earth's surface. HOMER assumes the output of the sun is constant in time. But the amount of sunlight striking the top of the earth's atmosphere varies over the year because the distance between the sun and the earth varies over the year due to the eccentricity of earth's orbit. To calculate the extraterrestrial normal radiation,

defined as the amount of solar radiation striking a surface normal (perpendicular) to the sun's rays at the top of the earth's atmosphere, HOMER uses the following equation:

$$G_{on} = G_{Sc}\left(1 + 0.033.\cos\frac{360n}{365}\right) \quad (2.22)$$

Where G_{on} is the extraterrestrial normal radiation [kWm^2]

G_{Sc} is the constant [1.367 kW/m^2]

n is the day of the year [a number between 1 and 365]

To calculate the extraterrestrial horizontal radiation, defined as the amount of solar radiation striking a horizontal surface at the top of the atmosphere, HOMER uses the following equation:

$$G_o = G_{on}\cos\theta_z \quad (2.23)$$

Where :

G_o is the extraerrestrial horizontal radiation [kw/m^2]

G_{on} is the extraerrestrial normal radiation [kw/m^2]

θ_z is the zenith angle[^{o}]

Since HOMER simulates on a time step by time step basis, we integrate the above equation over one time step to find the average extraterrestrial horizontal radiation over the time step:

$$\bar{G}_o = \frac{12}{\pi}G_{on}\left[\cos\phi\cos\delta\,(\sin\omega_2 + \sin\omega_1) + \frac{\pi(\omega_2-\omega_1)}{180^\circ}\sin\phi\sin\delta\right] \quad (2.24)$$

Where:

$\bar{G}_o$ is the extraterrestrial horizontal radiation averaged over the time step (kw/m^2]

G_{on} is the extraterrestrial normal radiation [kW/m^2]

ω_1 is the hour angle at the beginning of the time step[^{o}]

ω_2 is the hour angle at the end of the time step[^{o}]

The above equation gives the average amount of solar radiation striking a horizontal surface at the top of the atmosphere in any time step. The solar resource data give the average amount of solar radiation striking a horizontal surface at the bottom of the atmosphere (the surface of the earth) in every time step. The ratio of the surface radiation to the extraterrestrial radiation is called the clearness index. The following equation defines the clearness index:

$$k_T = \frac{\bar{G}}{\bar{G}_0} \tag{2.25}$$

Where:

$\bar{G}$ is the global horizontal radiation on the earth's surface averaged over the time step [kW/m^2]

$\overline{G}_0$ is the extraterrestrial horizontal radiation averaged over the time step [kw/m^2]

Now let us look more closely at the solar radiation on the earth's surface. Some of that radiation is beam radiation, defined as solar radiation that travels from the sun to the earth's surface without any scattering by the atmosphere. Beam radiation (sometimes called direct radiation) casts a shadow. The rest of the radiation is diffuse radiation, defined as solar radiation whose direction has been changed by the earth's atmosphere. Diffuse radiation comes from all parts of the sky and does not cast a shadow. The sum of beam and diffuse radiation is called global solar radiation, a relation expressed by the following equation.

$$\overline{G} = \overline{G}_b + \overline{G}_d \tag{2.26}$$

Where:

$\bar{G}_b$ is the beam radiation [kw/m^2]

$\bar{G}_d$ is the diffuse radiation [kw/m^2]

The distinction between beam and diffuse radiation is important when calculating the amount of radiation incident on an inclined surface. The orientation of the surface has a stronger effect on the beam radiation, which comes from only one part of the sky, than it does on the diffuse radiation, which comes from all parts of the sky.

However, in most cases we measure only the global horizontal radiation, not its beam and diffuse components. For that reason, HOMER expects you to enter global horizontal radiation in HOMER's Solar Resource Inputs window. That means that in every time step, HOMER must resolve the global horizontal radiation into its beam and diffuse components to find the radiation incident on the PV array. For this purpose HOMER uses correlation of Erbs et al. (1982), which gives the *diffuse fraction* as a function of the clearness index as follows:

$$\frac{\overline{G_d}}{\bar{G}} = \begin{cases} 1.0 - 0.09 \cdot k_T & for\ k_T \leq 0.22 \\ 0.9511 - 0.1604 \cdot k_T + 4.388 \cdot k_T^3 + 12.336 \cdot k_T^4 & for\ 0.22 < k_T \leq 0.8 \\ 0.165 & for\ k_T > 0.80 \end{cases} \quad (2.27)$$

For each time step, HOMER uses the average global horizontal radiation to calculate the clearness index, then the diffuse radiation. It then calculates the beam radiation by subtracting the diffuse radiation from the global horizontal radiation.

We are now almost ready to calculate the global radiation striking the tilted surface of the PV array. For this purpose HOMER uses the HDKR model, which assumes that there are three components to the diffuse solar radiation: an isotropic component which comes all parts of the sky equally, a circumsolar component which emanates from the direction of the sun, and a horizon brightening component which emanates from the horizon. Before applying that model we must first define three more factors.

The following equation defines R_b, the ratio of beam radiation on the tilted surface to beam radiation on the horizontal surface:

$$R_b = \frac{\cos\theta}{\cos\theta_z} \quad (2.28)$$

The anisotropy index, with symbol A_i, is a measure of the atmospheric transmittance of beam radiation. This factor is used to estimate the amount of circumsolar diffuse radiation, also called forward scattered radiation. The anisotropy index is given by the following equation:

$$A_i = \frac{\bar{G}_b}{\bar{G}_0} \quad (2.29)$$

The final factor we need to define is a factor used to account for 'horizon brightening', or the fact that more diffuse radiation comes from the horizon than from the rest of the sky. This term is related to the cloudiness and is given by the following equation:

$$f = \sqrt{\frac{\bar{G}_b}{\bar{G}}} \tag{2.30}$$

The HOMER model calculates the global radiation incident on the PV array according to the following equation:

$$\bar{G}_T = (\bar{G}_b + \bar{G}_d A_i) R_b + \bar{G}_b (1 - A_i) \left(\frac{1+\cos\beta}{2}\right) \left[1 + f \sin^3\left(\frac{\beta}{2}\right) + \bar{G}_{\rho_g} \left(\frac{1-\cos\beta}{2}\right)\right] \tag{2.31}$$

Where:

β is the slope of the surface[^{o}]

ρ_g is the ground reflectance, which is also called the albedo [%]

HOMER uses this quantity to calculate the cell temperature and the power output of the PV array.

2.4.6 Historical PV Pricing Trends

PV price is rated as $/Watt of the module. PV module factory prices (Appendix IV), have historically decreased from 2000 to 2014, IRENA 2014, [Appendix IV]. According to IRENA'S report [21], solar PV module prices in 2014 were 75% lower than their levels at the end of 2009. Detail price index is attached in the [Appendix IV].

Chapter Three

Load Estimation and Input Data to the Software

3.1 Methodology

The HOMER (Hybrid Optimization Model for Electrical Renewable) is used in this study as the modeling and simulation software for optimization and sensitivity analysis of the system. This software was developed by the US National Renewable Energy Laboratory (NREL).

3.2 Data Collection

Data for the HOMER software input has been collected from the following sources

i. Primary data

The primary Hydrological data for discharge, and the head for the un-gauged run-of river has been measured and collected on site. The discharge measurement for the un-gauged run-of river is done as per the manual of WMO No. 1029 "Manual on Low-Flow Estimation and Prediction" Operational Hydrology Report No. 50. , 2008) [3, 4, 7, 8]. A Velocity area Method procedure is implemented in the 3rd chapter, Flow Measurement.

ii. Secondary Data

Secondary data for wind, and solar radiation was collected from:

i. Ministry of water and Energy –flow rate of the river and GIS:
ii. Metrological wind data from NMAE (National Metrological Agency of Ethiopia,) for Debrebirhan wind station.
iii. Solar data has been down loaded from NASA.

3.3 Resource Assessment of Mini-Hydropower, Wind, and Solar Hybrid System

3.3.1 Assessment of Mini-hydropower of the site

i. Site Selection Criteria

In this project, the Ajana (Mugil Washa) river, which has a high head about 300m was measured. Access to the site, potential residents and the availability of other public facilities without electricity were checked.

On top of that, one of the most intensive criteria for selecting this river is that, the water is not controlled from the stream either for irrigation, dammed for drinking water or for any other purpose. Figure 3.1. shows river's location on the site. The Migul Washa / Ajana River site location is at 9°53'17.62"N and 30° 34'11.41"E [Source Google Mapper].

Figure 3.2. shows an overall view of the river with the surrounding landscape and part of the residents at bottom of the highland with the same site location.

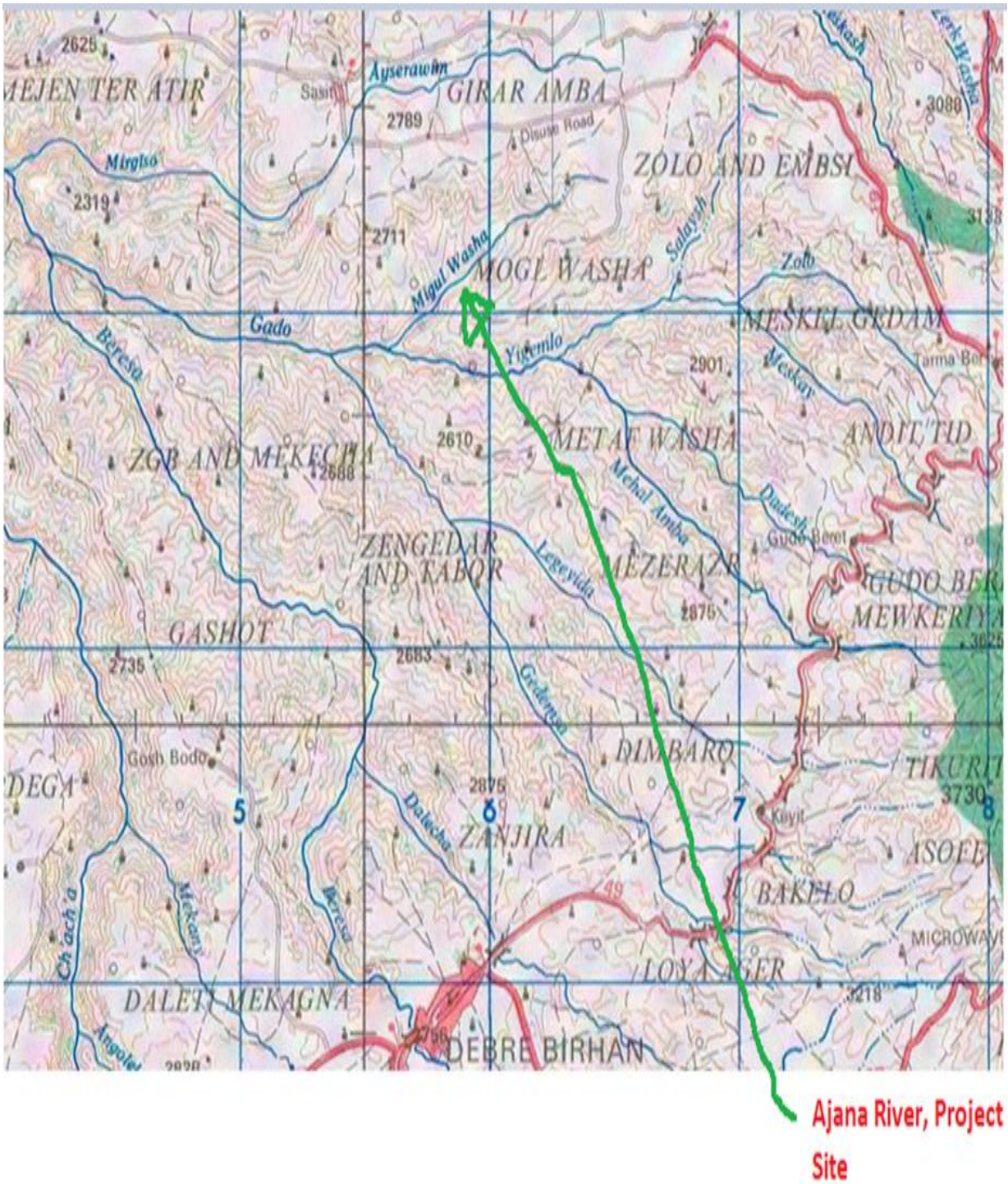

Figure 3.1 Rivers map of the site [Source Google Mapper]

\

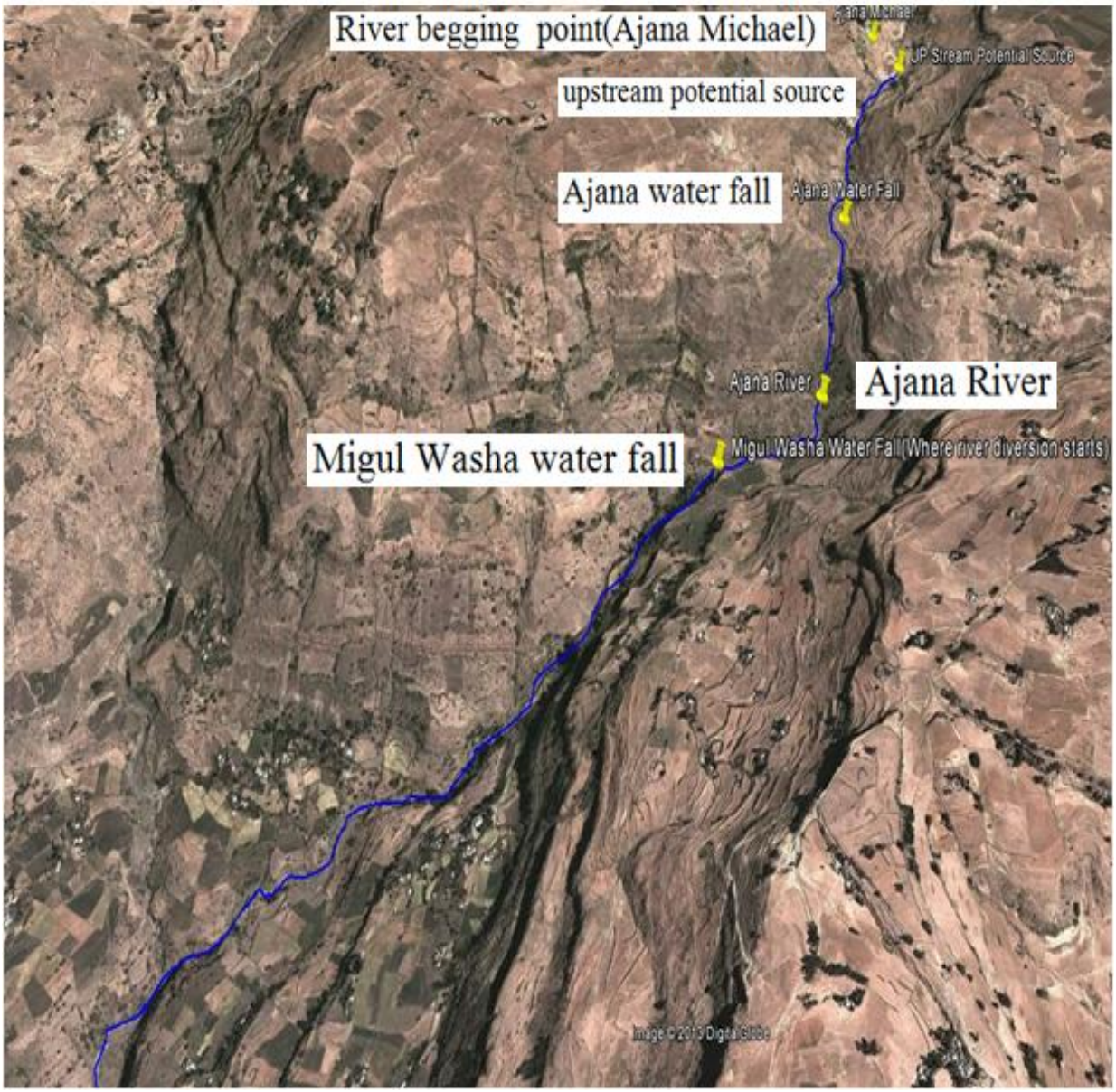

Figure 3.2 Over all view of the river with the surrounding landscape and part of the residents at bottom of the highland [source Google Mapper].

ii. Head Measurement

Though there are different methods for head measurement, in this project a GPS (Global positioning Systems) tool was used. The measured head is 300m. Two waterfalls with a height 45 and 25m respectively contribute almost more than one-fifth of the head of the water head. Figure 3.3. (a), (b), (c) shows the detail of what the two waterfalls of the river look like.

(a) (b) (c)

Figure 3.3 (a) The Ajana water fall is the first water fall of the potential head contributor, which is 45m high from top to the bottom of the fall; (b) The MigulWasha water fall is the second water fall in the project site is 25m high from the top to the diversion point, which is at the middle of the fall; (c) MigulWasha water fall, from a distance. The photo of the fall from the top of the fall to diversion starting point and the diversion point is half way of the water fall.

At the middle height of the second water fall, the water is diverted for irrigation. But, the diverted water is used for irrigation after having gone about 150m vertical height from the diversion point of the fall. The irrigation water passage way is an open ditch. Proposed turbine location is before the 100m vertical height from the starting point of the second water fall. The diversion point can be decided during the preparation of detail implementation plan.

iii. Flow measurement

Since there is no gauged data for this river, velocity-area method for un-gauged river has been used WMO No. 1029 “Manual on Low-Flow Estimation and Prediction” Operational Hydrology Report No. 50 , 2008) [8].Velocity area Method procedure is implemented as follows and as indicated in Figure 3.4 (a), and (b).

(a) (b)

Figure 3.4 Velocity measurement of the un-gauged river using velocity area method: (a) cross-sectional area measurement of the river and (b) Actual mean flow velocity measurement.

This flow rate measurement for the un-gauged run-of river had been taken at the highest dry month of the year, which is in May. Hence, flow rate data was collected on May 1, 2, and 30, 2013. Besides, additional data has been taken in November 15, 2013, and February 12, 2014. Measurement had been taken on the location where the river course is almost flat.

a. Velocity Measurement

Since it is an un-gauged run-of river, material used for float is a leaf of piece of Aloe "erate" for velocity measurement [3, 7, 8].The float material was supposed to travel for 6m length. The number of trials and the corresponding result is shown in the Table 3.1.

Table 3.1 Velocity of flow measurement for the un-gauged river.

No .of Trials	Time taken in min. for the float to cross the 6m line.
1	2:00
2	1:50
3	1:55
4	1:20
5	1:40

6	1:10
7	1:10
8	1:00
9	0.55
10	0.6
11	1.3
12	1:50
13	1:40
14	1:10
15	1:25
16	1:35
17	1:25
18	1:28
19	1:25
20	1:42

b. Cross- Section: Measurement of depth

The linear dimension of the cross-section for the river where the velocity measurement using a float is taken is 1.80m. The number of complete cross-section measurement is two and the averaged result is taken. The process is shown as per in the tabulated Table 3.2.

Table 3.2 Cross-section measurement with an interval of 10cm

Depth measurement interval at every 10 cm.	0	10	20	30	40	50	60	70	80	90	100
Measurement 1	47	51	56	59	61	63	66	68	66	40	32
Measurement 2	50	52	57	60	61	64	65	67	64	46	33

Depth measurement interval at every 10cm.	110	120	130	140	150	160	170	180
Measurement 1	35	30	27	21	16	7	7	0
Measurement 2	38	34	25	24	20	12	8	0

iv. Estimation of hydropower output of the site

From the above analysis, the stream flow for the site is estimated as follows [3]:

From the float and cross-section measurement [3]:

$u_s = 0.056\text{m/s}, \text{Aaverage} = 0.946m^2$

$$Q = V_{mean} \text{ x } A_{average} = 0.8 \text{ x } u_s \text{ x } A_{av} = 0.8 \text{ x } 0.056 \text{ x } 0.946 = 0.053\text{m}^3/\text{s} \quad (3.1)$$

From the above calculation, the design flow rate is taken $0.053\text{m}^3/\text{s}$ for simulation.

Hence, the output of hydropower of the site, for Q = 0.053m^3 /s , H= 300m, is 117kW.

3.3.2 Wind Resource Assessment of the Site

i. Methodology

Since the project site does not have measured wind speed data, different types of approaches has been taken for this site selection as wind valid data. Among those approaches are using SWERA'S GIS map, similar topography, and empirical. The GIS SWERA map of the wind pattern in the area, Figure 2.8 shows geographic distribution of wind resource in Ethiopia. According to SWERA's wind pattern map, this project site indicates a potential wind presence from 3.5 – 5.6m/s similar to that of Debrebirhan's [11]. In addition to that, according to professor Wolde-Ghiorgis, 1988, "Wind Energy Survey in Ethiopia", as per the result of his study, annual mean wind velocity greater than 2.8m/s is regarded as useful for small scale projects like this hybrid project site [22]. In both cases, this could be a valid wind potential to extract a small electrical power source from the available wind energy [11].

a. Similar topographic approach for wind data

Debrebirhan VS project site for the high land area: There is no main meteorological station in Seladingay, the nearest town to the project site where a sub-metrological wind station is available. But, it does not have main meteorological station with data for wind power. Hence, the nearest main wind station is at Debrebirhan, with altitude 2,818m, and with average annual wind speed 5.72m/s taken at the height of 10m above ground [11].

The project site under investigation is near the Ajana river and surroundings area, particularly Nech Gedel, the high land area of the project site, with an altitude of 2.860m has similarities in altitude, temperature, and rain fall to that of Debrebrihan. From an engineering experience the same altitude means similar temperature, similar soil type and similar rain fall. By this argument, Debrebirhan's 5 years of hourly measured wind is used as an input for the HOMER software.

b. Empirical approach

By visual inspection of the conditions of the trees in the project area, Nechgedel, the high land area part of the community, trees are bent in one direction due to presence of strong prevailing wind on the area as shown in Figure 3.5. This implies that vegetation is an indicator of potential wind presence [11].

Figure 3.5 Effect of prevailing wind on eucalyptus trees in project site.

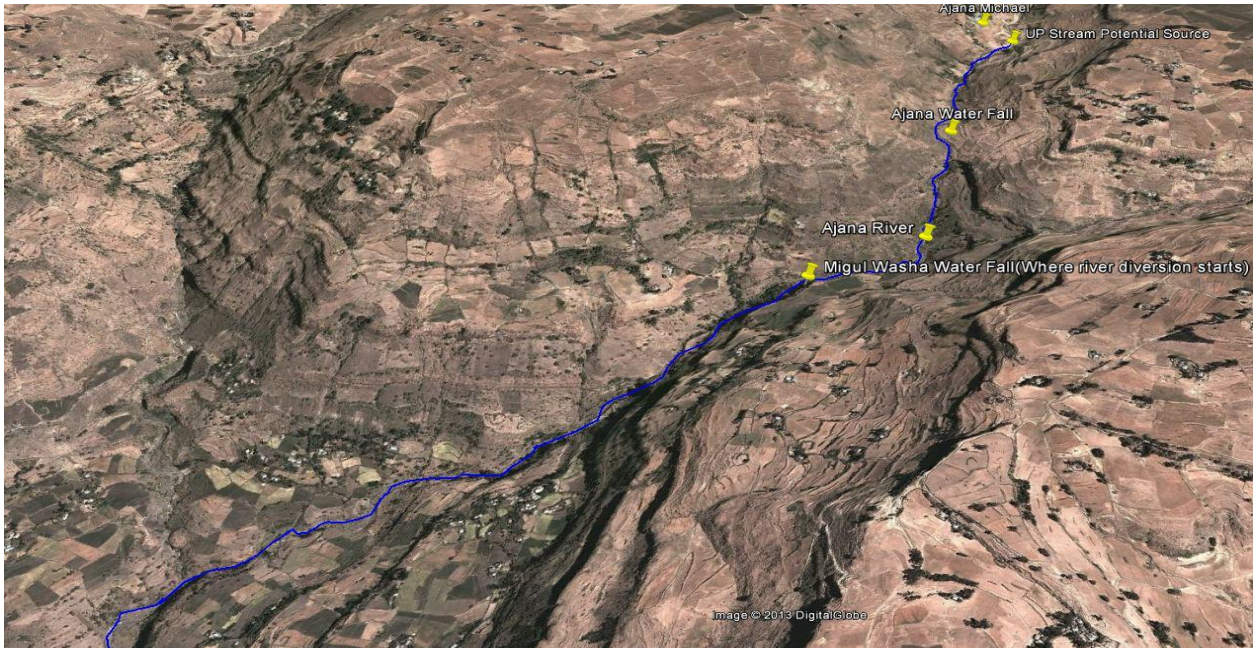

Figure 3.6 Project site favorable for the creation of mountain wind, Source Google Earth. Mountain wind is discussed in Chapter 2.3.3.

3.3.3 Solar Energy Assessment of Project Site

Data shown in the Table 3.3 is the monthly averaged radiation incident on an Equator-pointed tilted surface at 10deg. (kWh/m^2/day) [23]. The data in the table is used as an input for the software for solar power output estimation. This solar radiation data was obtained from NASA satellite measurements. The NASA data base was derived from the meteorology and energy parameters that have been recorded for 22 years by over 200 satellites. As an input for this thesis solar isolation on a horizontal surface and the regarding clearance index were used.

Table 3.3 Monthly averaged radiation incident on an Equator- pointed tilted surface at 10deg. (kWh/m^2/day) [23]

Month	Clearness Index [K]	Daily Radiation [kWh/m^2/Day]	Annual Average
Jan	0.66	6.36	
Feb	0.67	6.76	
Mar	0.65	6.77	

April	0.63	6.52	
May	0.62	6.46	
June	0.57	5.96	6.23
July	0.52	5.46	
Aug	0.54	5.62	
Sept	0.54	5.58	
Oct	0.6	6.12	
Nov	0.68	6.69	
Dec	0.69	6.53	

3.4 Load Estimation for the Villages under the Study

The total number of families without electricity in the vicinity of the river in the project site according to the Woreda's Administration legal document is 739 (Appendix VI: Population data by local administration office). Six persons per family are estimated. Hence, total size of people covered in this study is 4,434. Besides households, the following civil systems are operating in the project site: 2 schools from 1^{st} to 8^{th} grade containing from 800 to 1000 students each and teachers are dwelling within the school compound. Five churches with nuns, monks, and Yekolo Temari are living in the church compound. The following installations which are assumed to be built in the future are forecasted: Five flour mills, 2 milk processing plants, 2 health posts, and six water pumps as required except for churches are considered in the forecast. Based on this information, load forecast is tabulated as shown in Tables 3.4. to 3.6.The tabulation is divided as domestic and community.

Loads in this feasibility study are divided into two according to their nature, primary and deferrable. Primary load is an electrical load that must be met immediately and a deferrable load is an electrical load that must be met within some time period, but the exact time is not important. All considered loads are primary except water pumping. Water pumping is a deferrable load [14].

In this feasibility study, in addition to loads defined by Bekele G. [6], and Bekele and Getnet [15], additional loads are discussed as follows. For schools: lighting for teachers' residence, power for computers and the regarding accessories are added. For household, stove for

cooking is added in addition to Injera Mitad for baking bread. Two milk processing plants and electrical loads for five churches are included.

Detail description is given for each type of primary load in tabular form in Tables 3.4. to 3.6. except for the water pumping system's load. Water pumping considered as a deferrable load is discussed here [6, 16]. Ten water pumps with 300W power rating and pumping capacity of 20 liters/m are to be installed at appropriate locations for common use. The pumps operating for 6 hrs, supply 72,000 liters/day for 740 families (100 liters/family/day). For 2 schools, 2 health posts, and 2 milk processing plants, 6 pumps of 150W power rating, with operating time 5 hrs/day and 2400 liter/day/unit is proposed for each firm. Four days storage system is considered [6, 16]. For flour mill and churches, pumps are not proposed. Hence, the resulting total load is given in Table 3.7.

Figure. 3.7 (a) Regular lined up to begin mornings class. (b) Adult evening student studying by the help of kerosene lantern. Source: Project site's sample photos.

Table 3.4 Domestic Estimation. Appliance Energy Need

No.	Power Consumption	Power (watt)	Qty	Load (kW x qty x No. of H. Hold x Df=0.7)	Hr/Dy	kWh/day
1	Lighting(CFL)	11	3	17	5	85
2	TV	80	1	41.4	5	207

3	Radio	5	1	6.2	10	25
4	Stove	1000	1	258.6	3	775.8
5	Ingra Mitad	2500	1	426.7	2	853.4
6	Miscellaneous	20		10.3	24	247.2
	Total No. of household	739				
	Sub total			760.6		2,199.40

Table 3.5 Community (Public demand) service energy demand

	No.	Power Consumption	Power [W]	Qty	Load(Watt x Qty x No. of Schools x Df=0.6)	Hr/Day	kWh/day
School	1	Class room lighting (CFL)	15	15	0.27	3	0.81
	2	Office lighting (CFL)	11	10	0.132	3	0.396
	3	Teachers' residence lighting (CFL)	11	20	0.264	5	1.32
	4	Computer and Accessories	100	10	1.2	6	7.2
	5	Miscellaneous	30	30	0.036	24	0.864
		Total No. of Schools(From1st to 8th grade)= 2					
SUB-TOTAL					1.9		10.59
Agriculture	No.	Power Consumption	Power [Watt]	Qty	Load(Watt x Qty x No. of Schools x Df=0.6)	Hr/Day	
	6	Flour mill	7,500	5	30.0 (Df=0.8)	8	240
	7	Milk processing	4,000	2	6.48(Df=0.81)	4	25.92
Churches	No.	Power Consumption	Power[Watt]	Qty	Load(Watt x Qty x No. of Churches x	Hr/Day	

					Df=1)		
	8	Lighting (CFL)	15	5	0.375	4	1.5
	9	Megaphone	15	1	0.75	6	4.5
	10	Miscellaneous	20	1	0.01	24	0.24
		Total number of churches = 5					6.24

Table 3.6 Domestic Appliance (Health Post) Energy Estimation

No.	Power Consumption	Power (Watt)	Qty	Load (Watt x qty x No. of H. Post x Df=1)	Hr/Day	Remark
1	Lighting (CFL)	13	4	0.1	12	1.2
2	External Lighting (CFL)	23	1	0.446	12	5.4
3	Refrigerator	120	1	0.24	10	2.4
4	Microscope	20	1	0.04	7	0.28
5	Radio	12	1	0.24	16	3.84
6	Water Heater	1500	1	3	11	33
7	Ceiling Fan	100	4	0.8	12	9.6
8	Miscellaneous	20	1	0.04	24	0.96
	Total No. of Health Post = 2					
Sub Total				4.3		56.68

Table 3.7 Monthly average daily electrical Primary and Deferrable loads [kWh/Day].

Load Type Category	Demand (kWh/day)					
	Jan.	Feb. - May	June	July and Aug.	Sept.	Oct. – Dec.
Deferrable	20.7	22.5	20.7	20.7	22.5	22.5
Primary	1,402.80	1,418	1,418	1,402.80	1,418	1,418
Total	1,423.50	1,440.50	1,423.50	1,423.50	1,440.50	1,440.50

3.5 Modeling Hybrid Energy Systems

3.5.1 Introduction

Hybrid energy system is an excellent solution for electrification of remote rural areas where the grid extension is difficult and not economical. This type of system incorporates two or more renewable energy resources. Among these main renewable energy resources used in this study are: small/micro hydropower, wind, and photovoltaic (PV). Those energy resources when used in a hybrid system using energy producing components such as the PV module, hydro and wind turbines and other components to make the flow of energy complete(battery, inverter etc…), they provide smooth, reliable, uninterruptable, and cost effective electrical energy to the end users than if any of the system was used independently. This is because each system does not depend on the other to produce its own energy.

3.5.2 Standalone hybrid system

The standalone hybrid renewable energy system to be conducted in this thesis comprises a Mini-hydro, Wind, and PV with a generator set as a backup. A system component accessory such as storage battery and convertor is incorporated for the system to serve its purpose and for smooth and reliable operation. System architecture for a standalone hybrid renewable system that is suited for this thesis is shown in the figure 3.8. The DC Center mainly contains the charge controller.

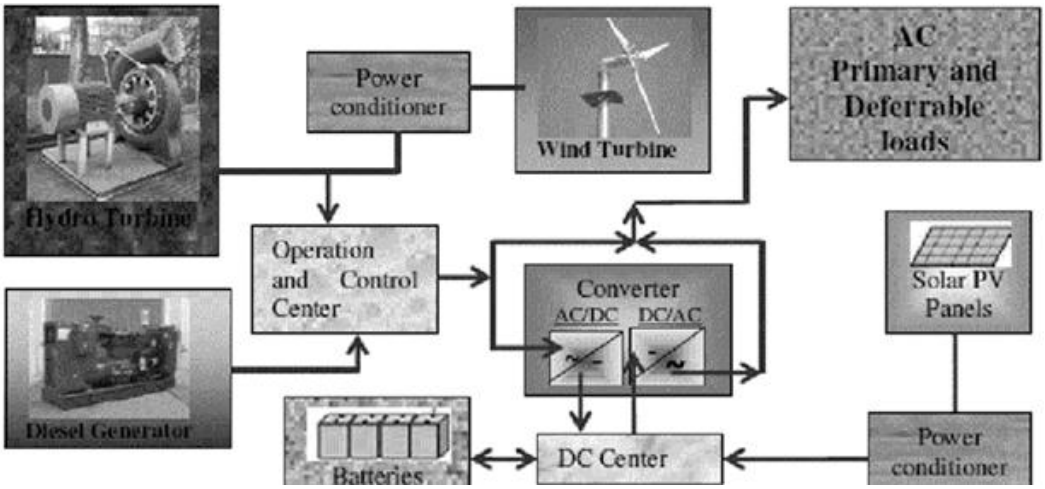

Figure 3.8 Typical hybrid system architecture standalone

3.5.3 Optimization of Hybrid Systems Using HOMER

Hybrid Optimization Model for Electric Renewable (HOMER) is a computer software developed by the US National Renewable Energy Laboratory (NREL) in 1992 [14]. It is a micropower optimization model and simplifies the task of evaluating designs of both off-grid and grid connected power systems for a variety of application. HOMER models a power system's physical behavior and its life cycle cost (Net Present Cost). That is the total cost of installing and operating the system throughout its life cycle. HOMER allows the modeler to compare many design options based on their technical and economic inputs [1, 17].

HOMER performs simulation, optimization, and sensitivity analysis in a single power system configuration. In a simulation process, HOMER simulates the operation of a system by making energy balance calculations for each of 8,760 hours in a year. For each hour, HOMER compares the electric demand in the hour to the energy that the system can supply in that hour, and calculates the flows of energy to and from each component of the system. It then determines whether the configuration is feasible and estimates the cost of installing and operating the system over the life time of the project. After simulating all of the possible system configurations, HOMER displays a list of configurations sorted by net present cost (NPC) or life cycle cost. This allows the modeler to compare design options. In the optimization process, HOMER simulates many different system configurations in search of the one that satisfies the technical constraints at the lower life cycle cost.

In the sensitivity analysis process, HOMER performs multiple optimizations under a range of input assumptions to gauge the effects of uncertainty or changes in the model inputs that the designer has no control [8, 23].

Data Input to HOMER

The following major inputs are given to the HOMER software, all in the regarding windows.

1. The un-gauged river's flow rate data is 0.053 cubic meter/sec and the regarding height is 300meters.
2. From National Metrology Agency's metrological data at 10m height, for 5 years annual average for each month.
3. Monthly averaged radiation incident on an Equatorial region - pointed tilted surface at 10deg. (kWh/m^2/day). Values for the software are from Table 3.3.
4. Primary and deferrable loads as per calculated.
5. Equipment cost for the regarding resource

After all the necessary inputs done to the software, HOMER converts the inputs to the graphical descriptions as shown from figure 3.9. to figure 3.16.

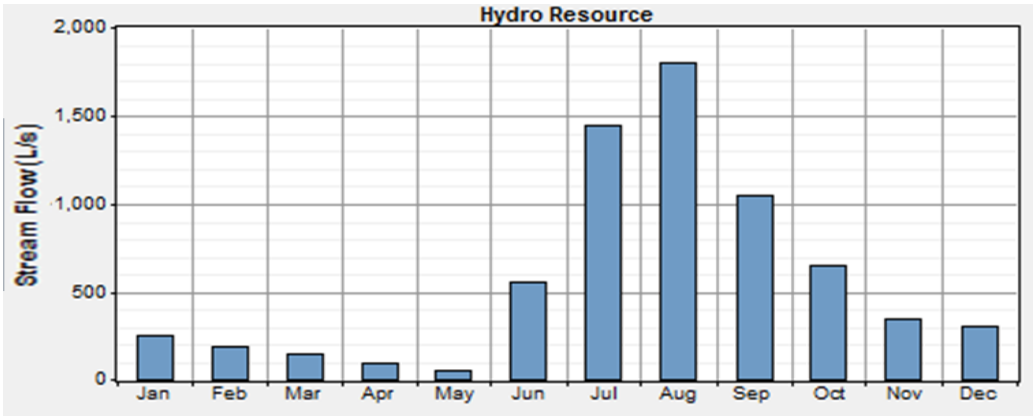

Figure 3.9 Annual Stream Flow of the un-guaged rever used as mini-hydro resource input

The stream flow data of Figure 3.9. is for the un-gauged run-of river [7, 8]. The data is taken in the 1st, 2nd, and 30th days of May [3], and November 15, 2013 respectively, and February 12, 2014. Though the flow in the stream varies with time, between draught and flood periods but for power generation we usually want to know the minimum dry season flow that is in the month of May. Since a turbine matched to this will produce power throughout the year. May's flow rate data is used as design flow rate for the software.

Five years monthly averaged wind speed data input to the software is presented in Figure 3.10. This data is for 10 meter's anemometer height. Additional inputs for the software with wind resource data are: Surface roughness length (m) 0.03. Weibull shape factor k=2, and autocorrelation factor c = 0.85 inserted by HOMER which corresponds to the input data.

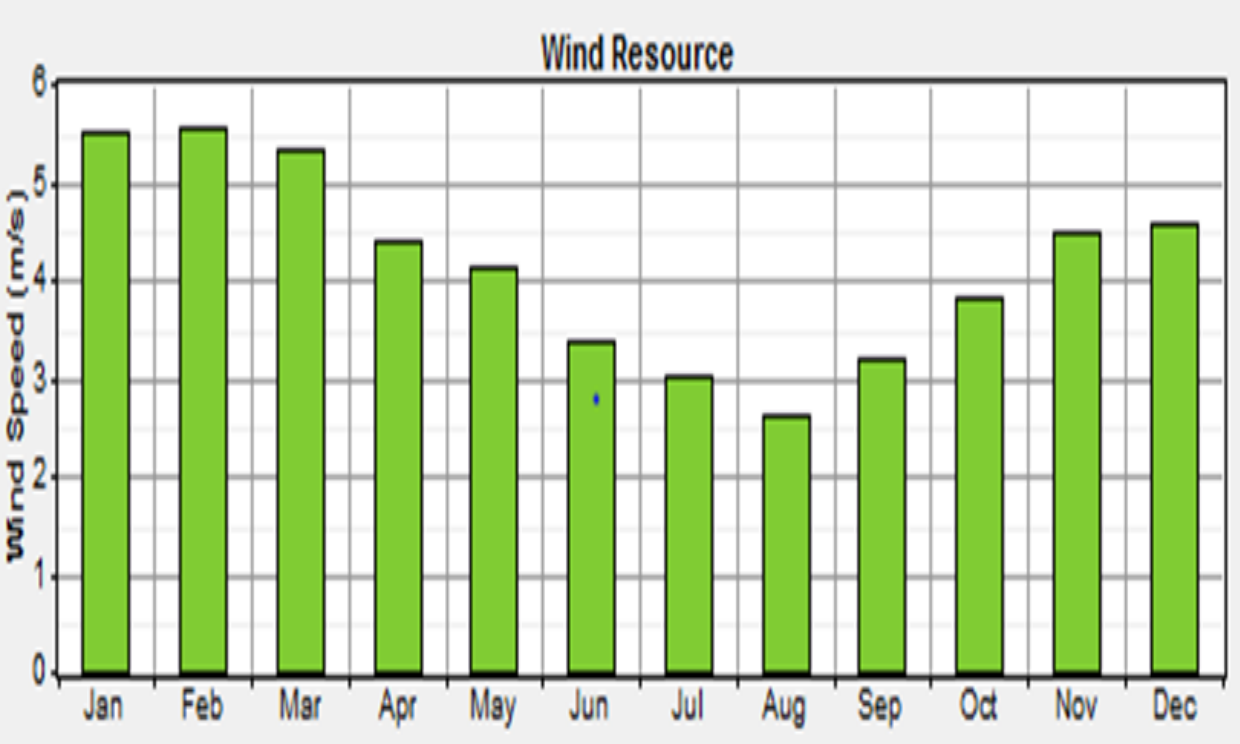

Figure 3.10 Five years monthly averaged wind Resource input. (Source: From National Metrological Agency.)

The HOMER synthesized probability density function at 10m height is shown in Figure 3.11. The type of wind turbine used is Eoltec Chinook E17-65. It has a good cut-in speed of 2.3m/sec. Its power curve is shown in Figure 3.12. The cut-in speed is 2.3m/sec.

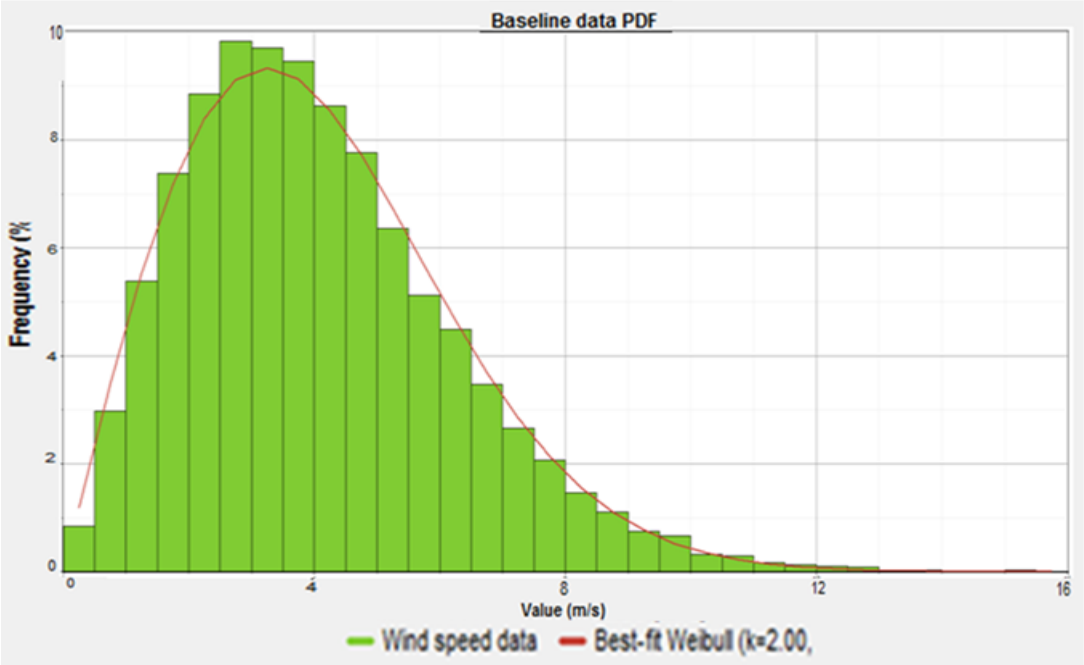

Figure 3.11 Probablity density vs wind speed at 10m hub height.

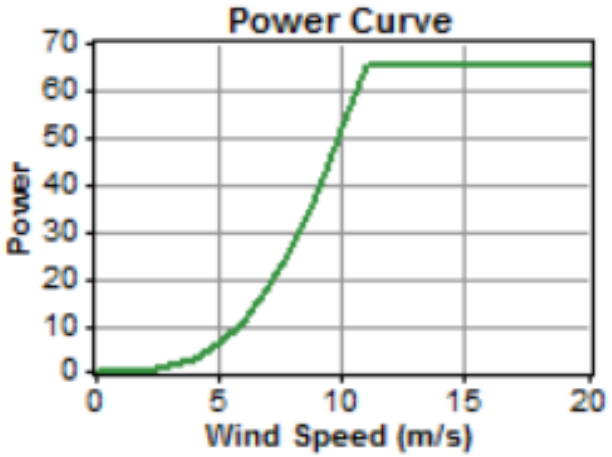

Figure 3.12 Eoltec Chinook Wind Turbine Efficiency Power Curve

Solar insulation data is presented in figure 3.13. Clearance index is low from mid June to mid of September due to rain and cloudy days of the rainy season for those months. Annual average solar insolation is 6.23kWh/m^2 /day.

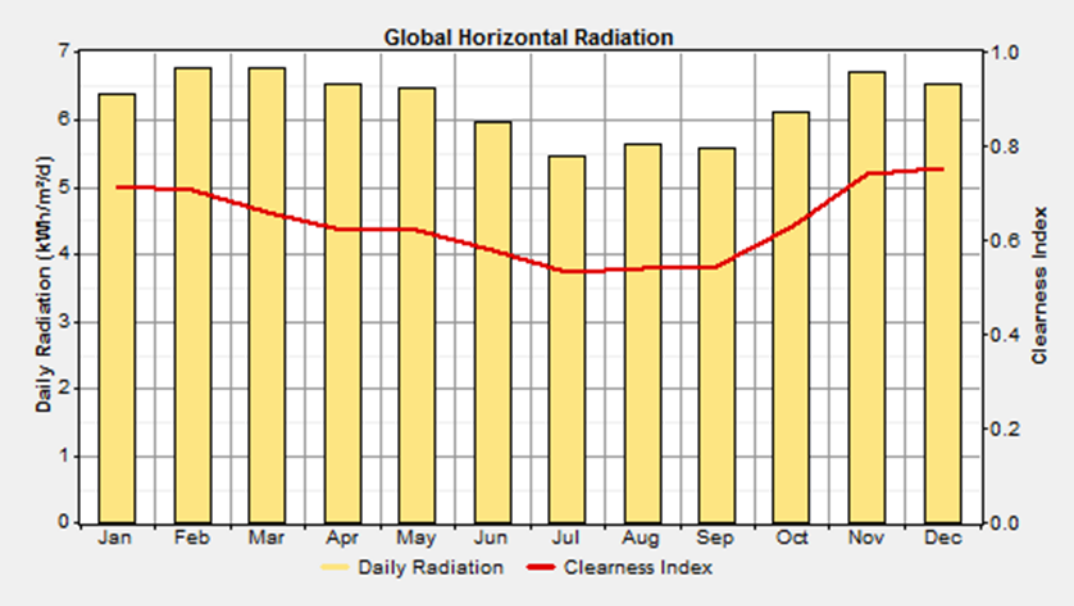

Figure 3.13 Solar Radiation input: Monthly Averaged Solar Radiation (kW/m$^{2/}$/day)

Diesel generator is allowed to operate under a minimum load ratio of 70%. Its fuel curve characterstics are calculated by HOMER. The generator's efficiency versus its percentage load is shown in figure 3.14. A Diesel price of $1/L, $1.5/L, and $2/L is considered. For 100% power output of the generator, the maximum efficiencay is 35%.

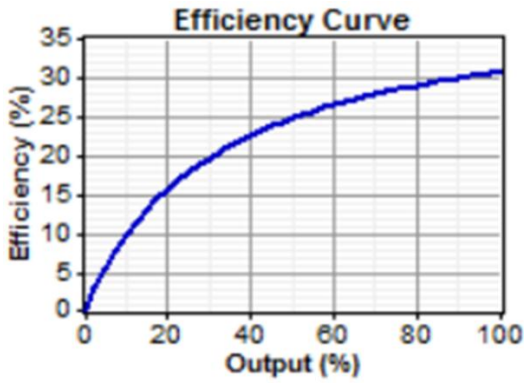

Figure 3.14 Diesel Generator Efficiency Curve

One of the inputs to the software is load. Having determinining the hourly community electric load for the primary and the deferrable load types, the monthly average of the daily load is supplied to the software. The load profiles are shown in figure 3.15 and figure 3.16.

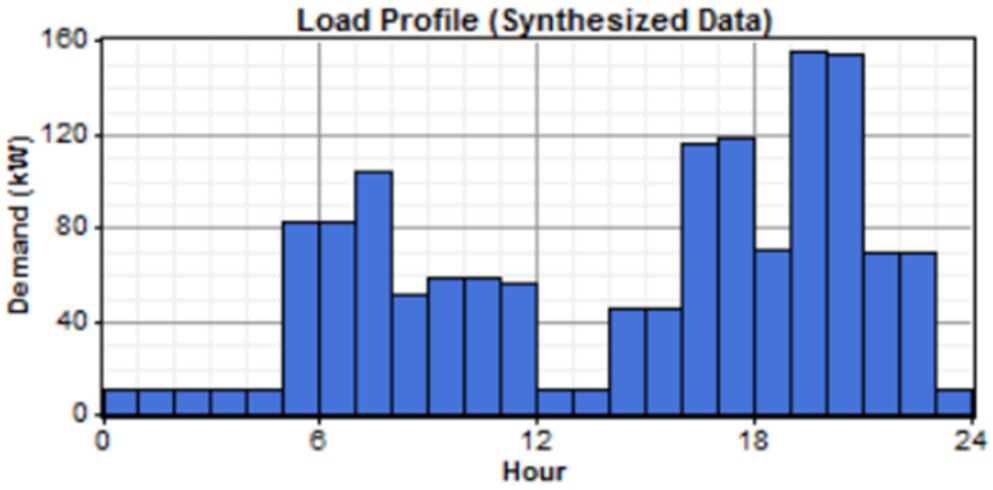

Figure 3.15 Overall system daily primary load profile shown by the software.

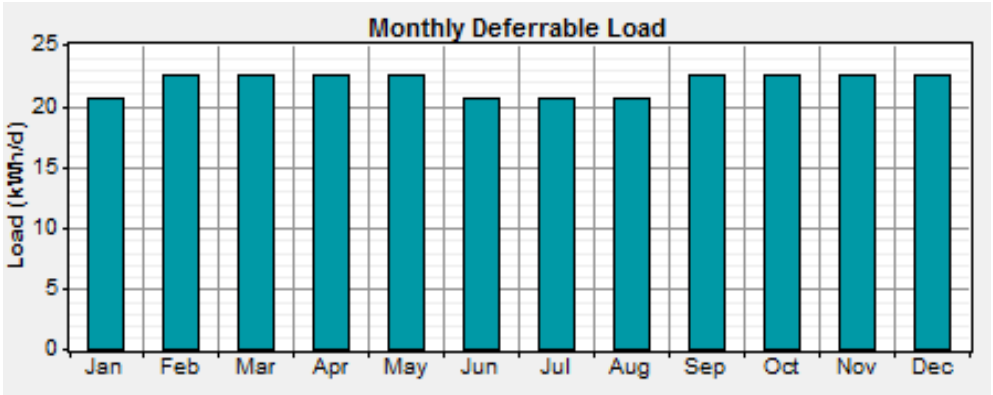

Figure 3.16 Overall system deferrable load input is converted from tabulation to bar chart by the software.

Additional data input to the software is summarized in Table. 3.8.

Table 3.8 Additional data input to HOMER Software

	Module PV	Wind turbine	System Hydro	Generation Diesel	Battery S6cs 25p	Converter
Size(kW)	160	65	117	1	1156Ah	1
Capital ($)	750 - 1200	65,000	160,000	0-1500	840	600
Replacement Cost ($)	400-800	45,000	120,000	0-1000	450	400
O&M cost($/yr)	0-25	300	3,500	0.4$/hr	16	10

3.5.4 Simulation Setup

The DC power produced by the PV array is converted in to AC and fed to the AC bus. The AC power generated from Hydro turbine, Wind turbine, and AC generator directly fed to the AC bus and fed to the AC loads. Excess power goes to the Battery bank and utilized by the system in case of lack of power by Hydro, Wind, and PV sources. The system architecture simulated by HOMER is shown in figure 3.17. Hydro/Wind/ PV Hybrid System Architecture.3

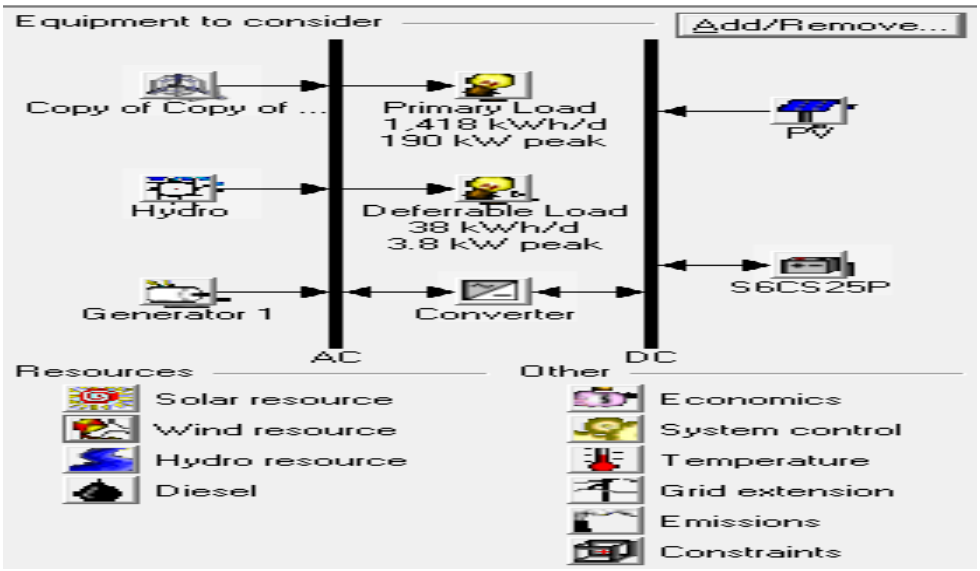

Figure 3.17 Hydro/ Wind/ PV Hybrid System Architecture

Chapter Four

Result and Discussion

4.1 Result and Discussion

The necessary input data discussed in the previous section to run the software has been given and the simulation program was completed. The feasible results are offered in the form of schemes ranked on the bases of NPC (Net Present Cost), from the lowest to the highest. The purpose of the feasibility study is to ensure if the available renewable resources as a hybrid system are quite enough to fulfill the power demand of the communities' requirement. The result list of optimal combinations of realized setups obtained is shown both in categorized and overall form. The overall table extraction is based on the renewable resources contribution in the realized setup.

The categorized table is the result of each component's contribution according to the Initial Capital, NPC, and COE with the ascending order of rank. In both tables optimization results, rank number one is the most optimized system with least COE of 0.056$/kWh. The most optimized hybrid system's result is with 100% renewable fraction of Mini-hydro and Wind, without PV and generator set. The contribution from the Solar PV system is 160 kW, which comes in rank of 107 with NPC and COE of 249% to that of the most feasible result rank number of 1. There is no generator's contribution up to the rank of 200. Hence, the PV and generator are smallest contributors to the most cost effective feasible hybrid system.

Table 4.1 Extracted from the categorized optimization results list

Rank	Hydro (kW)	Wind Turbine (No.)	PV (kW)	Gen (kW)	Battery	Converter (kW)	Dispatch Strategy	Initial Capital ($)	Total NPC ($)	COE ($/kWh)	Refraction	Diesel (L/yr)	Gen (hrs/yr)
1	117	1	0	0	60	50	CC	289,400	374,131	0.056	1	0	0
2	117	0	0	0	100	60	CC	292,000	396,217	0.6	1	0	0
3	117	1	160	0	60	50	CC	641,400	930,517	0.14	1	0	0
4	117	0	160	0	100	60	CC	644,000	952,480	0.14	1	0	0
5	117	1	0	60	60	70	LF	395,400	1,159,486	0.17	0.9	15,28	1,58
6	117	0	0	60	100	70	LF	390,000	1,190,746	0.175	0.96	15,353	1,640

7	117	1	160	60	60	70	LF	747,400	1,715,509	0.253	0.97	15,270	1579
8	117	0	160	60	100	70	LF	742,000	1,746,977	0.257	0.96	15,351	1,640
9	117	3	300	120	150	70	LF	1,139,000	5,217,235	0.776	0.7	88,201	3,901

Table 4.2 Extracted from the overall optimization results list

Rank	Hydro (kW)	Wind Turbine (No.)	PV (kW)	Gen (kW)	Battery	Converter (kW)	Dispatch Strategy	Initial Capital ($)	Total NPC ($)	COE ($/kWh)	Refraction	Diesel (L/yr)	Gen (hrs/yr)
1	117	1	0	0	60	50	CC	289,400	374,131	0.056	1	0	0
7	117	2	0	0	40	50	CC	311,600	388,263	0.058	1	0	0
13	117	0	0	0	100	60	CC	292,000	396,217	0.06	1	0	0
32	117	3	0	0	40	40	LF	342,600	421,688	0.063	1	0	0
107	117	1	160	0	60	50	LF	641,400	930,517	0.14	1	0	0
113	117	2	160	0	40	50	LF	663,600	944,708	0.142	1	0	0
120	117	0	160	0	100	60	LF	644,000	952,480	0.143	1	0	0

As it is shown in the monthly electric production result Figure 4.1, for the most optimum feasible system, with a renewable refraction of 100 percent, the main energy contributor is hydro with 82 percent, and the next is wind with 18 percent. The mini-hydro share is uniform throughout the year. Because, the un-gauged stream data for the minimum flow month in May, was collected and used input to the software as design flow discharge. Solar contribution is ranked at 107 on Table 4. 2. Hence, from the result it shows is that there is not much utilizable solar energy in the area. Besides the generator, it is not in one of the front lines optimum options. What can be understood from the software's result, is that the contribution from hydro and wind is satisfactory to carry out the 24 hours, 100% electrical energy demand of the community.

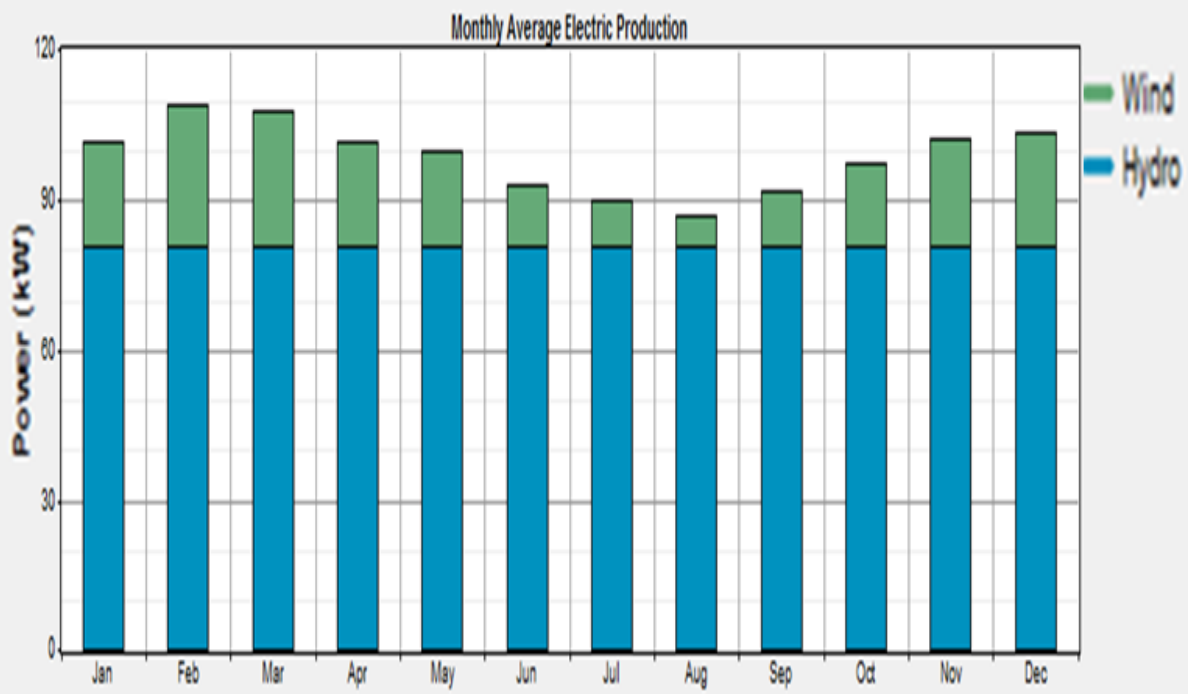

Figure 4.1 Monthly average electric production result for the most optimized system and with 100% hybrid renewable energy

From electrical load forecast tables, the total calculated daily energy load demand is 2,538.83kWh/day. The average total primary and deferrable daily load demand as per the result of the HOMER software is 1,456.0kWh/day. The percentage of daily average is 57.3%.

The system is also simulated in order to evaluate its operational characteristics, such as annual electric energy production, annual electric energy consumption, excess electricity, unmet electric load, capacity shortage, and renewable energy fraction. Table 4.3 shows the overall system report with input data of: Global solar radiation 6.23 kWh/m^2 /day, and wind speed of 5.72m/sec. Diesel fuel price is assumed to be $1/litter, and Eoltec wind turbine capital multiplier of 0.6.

Table 4.3 System report for 100% renewable energy resource

Sensitivity Case	
Design flow rate	0.053m³/s
Stream flow rate	0.053m³/s
Wind data	5.72m/s
Solar data	6.23kWh/m2 /day
PV capital cost multiplier	0.6
PV replacement cost multiplier	0.6

System Architecture	
Hydro	117kW
Wind Turbine	1x65kW
PV	0
Generator	0
Battery	60
Convertor	50

Annual electric production		
(kWh/yr)		
Hydro turbine	706,775	82%
Wind turbine	156,381	18%
PV array	0	
Generator	0	
Access electricity	325,821	37.70%
Unmet load	9,914	1.90%
Capacity shortage	20,879	3.90%
Renewable fraction		100%

Annual electric energy consumption(kWh/yr)		
AC primary load	507,657	97%
Deferrable load	13,757	3%
Total	521,414	100%

Cost summary	
Total NPC	$374,131
Levelized COE	0.056$/kWh
Operating cost	6,628$/yr

Emission	
(kg/yr)	
CO_2	0
CO	0
Unburned	0
Particulate matter	0
SO_2	0
NO_x	0

The cash flow summary from the result of the software, for most optimum system according to the NPC is shown in the Figure 4.2. The components are 1 wind turbine, 117 kW Pelton hydro turbine, 60kVA battery and 50kW convertor, respectively.

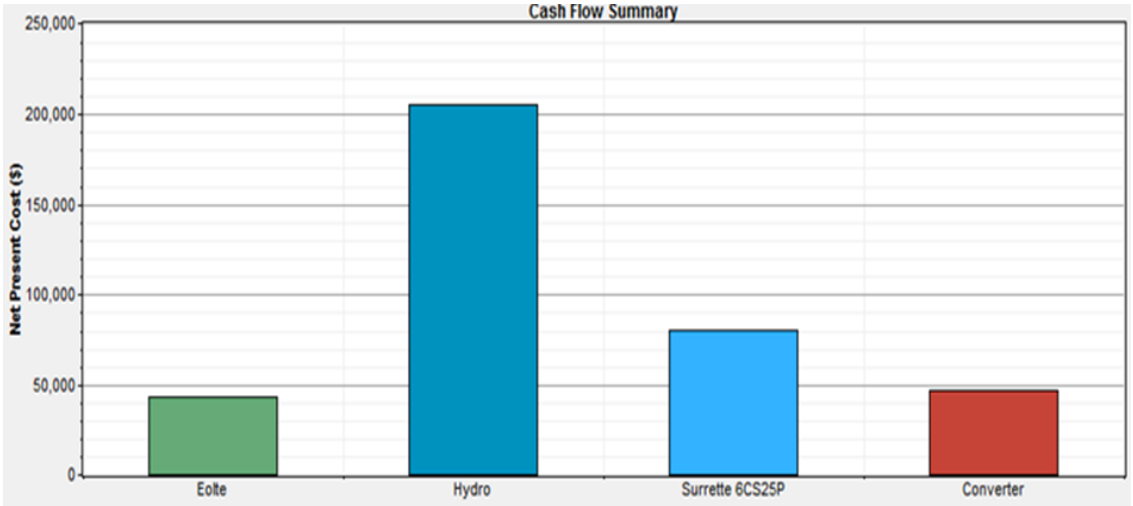

Component	Capital ($)	Replacement ($)	O&M ($)	Fuel ($)	Salvage ($)	Total ($)
Eoltec ChinookE 17-65	39,000	0	3,835	0	0	42,835
Hydro	160,000	0	44,742	0	0	204,742
Surrette 6CS25P	50,400	21,914	12,272	0	-4,423	80,162
Converter	40,000	0	6,392	0	0	46,392
System	289,400	21,914	67,240	0	-4,423	374,131

Figure. 4.2 Cash flow summary of the most feasible optimum system

The sensitivity analysis is also carried out. Figure 4.3 describes variation wind capital cost multiplier against Diesel fuel price. With varied Diesel fuel price and wind turbine capital cost multiplier between $0.6 and $0.95, Hydro/Wind/Battery is cost effective. On the other hand, if the wind capital cost multiplier is greater than $0.95, hydro/battery is optimal. From the sensitivity result in Figure 4.3, when wind turbine price multiplier is greater than 0.95, hydro and battery is optimal but, with higher battery size from 60 in rank 1 to 100 in rank 13. As a result the NPC escalates from $374,131 to $396,217. Since the PV and Diesel generator do not contribute to the most optimum system, they do not appear in the sensitivity figure.

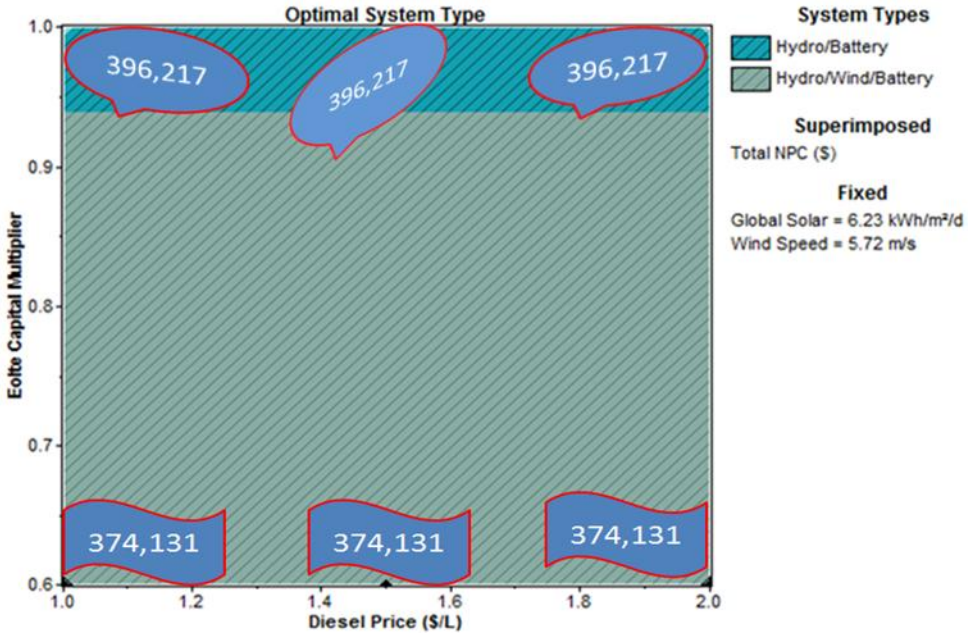

Figure 4.3 Sensitivity of Wind capital cost to Diesel price

4.2 Economical Comparison of Off-grid System Versus Grid Extension

Breakeven distance is the distance from the grid which makes the NPC of the grid extension equal to the NPC of the off-grid system. If the grid is further away from this breakeven distance, the off-grid system is optimal and if the grid is nearer to the breakeven distance, grid extension is optimal, and vice versa. This shows that grid extension prices are distance dependent.

EEPCo.'s substation is at Debrebirhan which is 82km away from this thesis's project site. There is no other substation nearer to the project site. Hence, economical grid extension comparison from the Deberebirhan substation against the off-grid system of this project site is computed. The unit cost for 33kV transmission line extension is $25,000/km, with 2% operation and maintenance cost is $500/km/year of capital cost. The village under the study for the project site is 82km away from the Debrebirhan substation. Therefore, the total capital cost of grid extension to cover 82kM is $2,091,000. Therefore, according to the result of the software simulation, in Figure 4.4., off-grid power supply system is the optimum and economical solution for those villages.

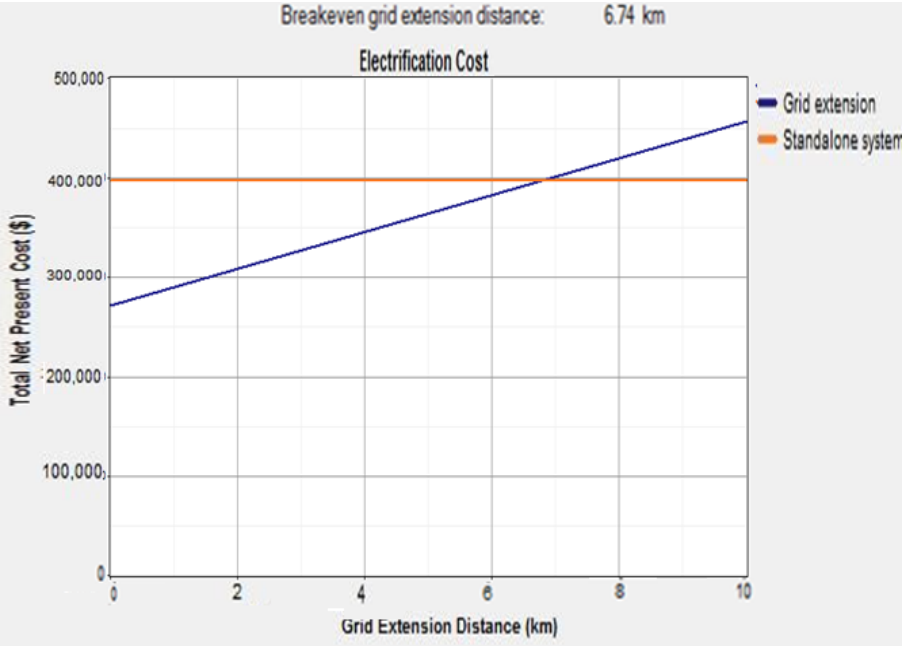

Figure 4.4 Economical comparison of grid extension versus off- grid system

Chapter Five

Conclusion and Recommendation

5.1 Conclusion

The most cost effective optimum renewable hybrid energy resources are hydro and wind which contain 82% and 18% of the total share respectively. The hybrid system is 100% renewable. Therefore, no emission. This thesis's hybrid renewable cost of energy is 0.056 USD/kWh on the higher side to that of the conventional grid's cost 0.04USD/kWh. This grid cost is for large hydropower. The world's trend for small projects COE/kWh is usually higher than that of large projects. A number of studies and simulations have been carried out that show the comparative costs of renewable energy systems as well as their competiveness with conventional energy options. As it is shown in the price index for wind and PV systems, prices for those systems are dramatically falling from previous years. This shows that hybrid renewable systems will be cost effective and competitive in the near future.

Extra costs such as: soil study, land survey, design cost, cost of tunnel/ ditch, cost of water passage system, and profit and overhead are not included in this feasibility study, because, the focus of this thesis is to find feasible solution of renewable resourced based hybrid electricity supply system to community without reach to the national grid.

Even though this study focuses on this community size, the excess electricity can be used for the nearby villages if it is extended. The unmet load is only 1.9%. This shows shortage of electricity is minimal.

5.2 Recommendation

From the result of the research, it is realized that this area is rich in renewable resources. It contributes to assure sustainable and quality life to those remote rural people in this district and could be applicable to other similar areas with same climate. What is required is to have a scientific measurement data stations for the un-gauged run-of river discharge and wind speed measurement for long years. This can help to know the exact utilizable energy potential of the resources of the site based on scientific base data.

This thesis can be used as reference material for further studies for students in the area. It can initiate policy makers, government or NGOs implementing rural electrification programs

either in this district or in other similar climatological parts of the country. It motivates the people living in this remote area to push government authorities for access to electricity.

5.3 Suggestions for Future Work

Existing traditional irrigation water passage of the project site should be upgraded, modified, and extended as required to a level that could be used both as mini open hydro canal and irrigation. Figure 5.1 is a sample concept, experience from other countries [4]. Leading water to fore bay is chosen because the project's landscapes are very similar. Besides, open canal is cheap by comparison. very similar. Besides, open canal is cheap by comparison.

Figure 5.1 Sample concept, experience from other countries [10]

Reference

1 Deepak Kumar Lal, November 3, 2011. Optimization of PV/wind Micro- Hydro/Dieses/ Hybrid power System in HOMER for the study area, International Journal on Electrical Engineering and Informatics, volume 3,

2 EEPCo. 2011, Annual Report

3 John Tewidell and Tony Weir, 2006. Renewable Energy Resource: second Edition:Tylor &Francis Group, London and New York:

4 JICA, 2009, Manual for Micro-hydropower Development, in Rural Electrification, Volume 1

5 S. Ashok, July 2006. Optimization model for community- based hybrid energy systems, ELSEVIER

6 Getachew Bekele, 2011, Feasibility Study of Solar- Wind Based Standalone Hybrid System for Application in Ethiopia: Addis Ababa Institute of Technology, Addis Ababa university Addis Ababa, Ethiopia; World Renewable Energy Congress - Sweden; getachew @ ece. Aau.edu.et, getachewbk@yahoo.com

7 ESHA, 2 2007, Small Hydro Power Development in Africa 'EIS Africa Issue. Guide on How to Develop a small Hydro power plant. European Small Hydropower Association – ESHA-esha @arcadis.de

8 WMO No. 1029, 2008, Manual on Low-Flow Estimation and Prediction" Operational Hydrology Report No. 50. ,

9 Manufacturer Of Hydraulic Turbines, Manufacturer of Hydro turbines turbines@leffelcompany.com

10 Erich Hau, 2006, Wind Turbines, 2nd edition, Springer, UK

11 TERNA, April 2005, Wind Energy Programme, Site Selection Report Ethiopia: Deutsche Gesellschaft fur Technische Zusammenarbeit (GTZ) GmbH- Wind Energy Programme TERNA, intemet: http:www.gtz. De/wind; e-mail: jasper. Abramowski @ grz. De

12 Sathyajith Mathew, 2006, Wind Energy Fundamentals Resource Analysis and Economics, Netherlands, p61 – 95,

13 HOMER Software, 2011, help index. WWW.homenergy.com

14 HOMER, 2011, The Micropower Optimization Model, WWW.homenergy.com, 2011

15 Bekele, Getenet, May 2011, Feasibility study of Small-hydro, PV, and Wind Hybrid System for Off-grid Rural electrification in Ethiopia, Journal ELSEVIER.
16 Md. Abu Saakalyen, Feb. 2013, Integrated Analysis of Hybrid System for Electrification of Isolated Island in Bangladesh, Canadian Journal on Electrical Electronics Engineering, Vol. 4, No. 1
17 Paul Gilman, 2006, Micro-power system modeling with HOMER, National Renewable Energy Laboratory
18 Florida Solar Energy Center, University of Florida, WWW.fsec.ucf.edu
19 Solar Photovoltaic Technologies, WWW.solarbuildingtech.com
20 Output Photovoltaic Array Power, Reference Books
21 IRENA, 2014, Power Generation Costs, 2014
22 Wolde Ghiorgis, 1988, Wind Energy Survey in Ethiopia
23 NASA, Surface Metrology and Solar Energy
24 International Journal of Immerging Technology and Advanced Engineering. WWW.ijetae.com, Volume 3, Issue 3, March 2013.

List of Appendixes

Appendix I

Load Scheduling for the Village

a) Domestic Appliance[kW]

Time	1	2	3	4	5	6	Total
00-01						10.4	10.4
01- 02						10.4	10.4
02- 03						10.4	10.4
03- 04						10.4	10.4
04 -05						10.4	10.4
05 -06					71.1	10.4	81.5
06- 07					71.1	10.4	81.5
07 -08			6.2	86.2		10.4	103
08 -09			6.2			10.4	16.6
09 -10			6.2			10.4	16.6

10- 11			6.2			10.4	16.6
11 -12			6.2			10.4	16.6
12 -13						10.4	10.4
13 -14						10.4	10.4
14 -15						10.4	10.4
15 -16						10.4	10.4
16 -17					71.1	10.4	81.5
17 -18					71.1	10.4	81.5
18 -19	17	41.4				10.4	68.8
19 -20	17	41.4		86.2		10.4	155
20 -21	17	41.4		86.2		10.4	155
21 -22	17	41.4				10.4	68.8
22 -23	17	41.4				10.4	68.8
23 -00						10.4	10.4

b) Public + Health Posts Load Schedule with total Domestic and overall project load [kW]

Time	1	2	3	4	5	6	7	8	9	10	Public + Health	Domestic	Project Load
00-01	0.104	0			0			0.02		0.1	0.306	10.4	10.706
2-Jan	0.104	0			0			0.02		0.1	0.306	10.4	10.706
3-Feb	0.104	0			0			0.02		0.1	0.306	10.4	10.706
4-Mar	0.104	0			0			0.02		0.1	0.306	10.4	10.706
5-Apr	0.104	0			0			0.415	0.075	0.1	0.756	10.4	11.156
6-May	0.104	0			0			0.415	0.075	0.1	0.756	81.5	82.256
7-Jun					0			0.02	0.075	0.1	0.231	81.5	81.731
07 – 08			0.1		0	1.5		0.02		0.1	1.776	103	104.78
9-Aug			0.1	1.2	0	33		0.02		0.1	34.508	16.6	51.108
10-Sep			0.1	1.2	0	33	6.6	0.02		0.1	41.88	16.6	58.48
11-Oct			0.1	1.2	0	33	6.6	0.02		0.1	41.88	16.6	58.48
12-Nov			0.1	0	0	33	6.6	0.02		0.1	39.888	16.6	56.488
13-Dec			0.1		0		0.1	0.02		0.1	0.388	10.4	10.788
13 -14			0.1	0	0		0.1	0.02		0.1	0.408	10.4	10.808
14 -15			0.1	1.2	0	33	0.1	0.02		0.1	34.608	10.4	45
15 -16			0.1	1.2	0	33	0.1	0.02		0.1	34.608	10.4	45
16 -17			0.1	1.2	0	33	0.1	0.02		0.1	34.608	81.5	116.11
17 -18			0.1		0		0.1	0.02		0.1	39.388	81.5	120.89

18 -19	0.374	0.2	0.3		0			0.395	0.075	0.1	1.432	68.9	70.232
19 -20	0.374	0.2	0.3		0			0.395	0.075	0.1	1.432	155	156.43
20 -21	0.374	0.2	0.3		0			0.02	0.075	0.1	1.432	155	156.43
21 -22	0.104	0	0.3		0			0.02		0.1	0.582	68.8	69.382
22-23	0.104	0	0.3		0			0.02		0.1	0.582	68.8	69.382
23-00					0					0.1	0.136	10.4	10.536

Appendix II

Wind turbine specification

Table 2.6: Technical Data of EOLTEC CHINOOK 17-65 Wind Turbine

Technical Data of EOLTEC CHINOOK 17-65 Wind Turbine	
Rated power	65 kW @ 10 m/s
Cut-in wind speed	2.3 m/s
Cut-out wind speed	20 m/s
Rated wind speed	11 m/s
Survival speed	50 m/s
Number of rotor blades	3
Rotor diameter	17 m
Swept area	227 m2
Rotor speed (variable)	25-75 rpm
Power control	Active blade pitch control
Hub height 32-40 m	(40 m is used for simulations)

Appendix III

Wind Turbine Price Index

Figure 42: Capex – wind turbine price index by turbine type and delivery date, 2008-12 ($m/MW)

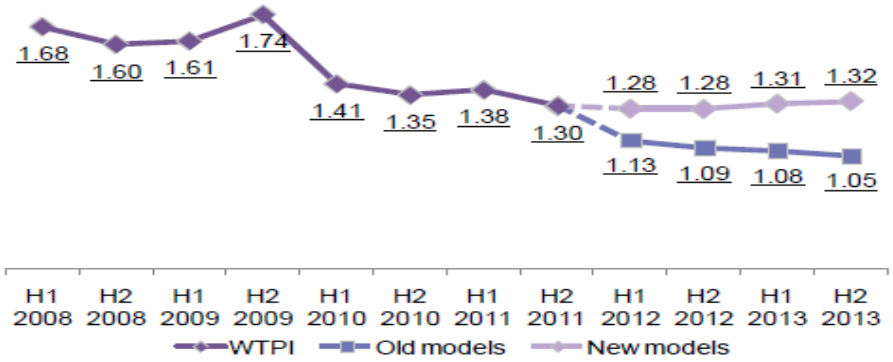

Source: Bloomberg New Energy Finance Notes: Global Wind Turbine Price Index converted to from EUR to USD by the average EUR/USD rate for the half year of turbine delivery.

Appendix IV

PV Price Index

FIGURE 2.2: CUMULATIVE GLOBAL SOLAR PHOTOVOLTAIC DEPLOYMENT AND SOLAR PHOTOVOLTAIC MODULE PRICES, 2000 TO 2014

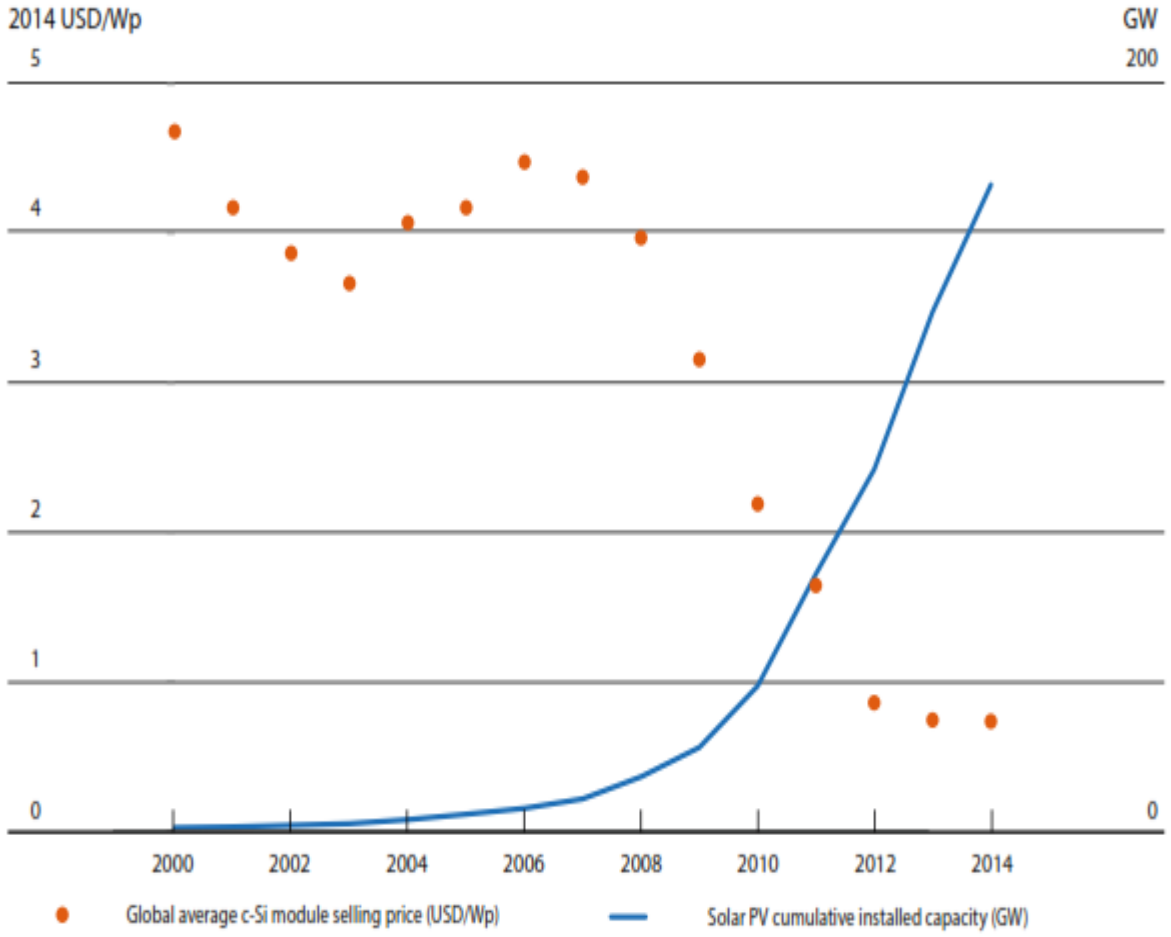

Sources: IRENA and pvXchange, 2014.

Price of c-Si PV module experience curve ($/W)

Figure 36: Capex – best-in-class cost of global utility-scale PV, 2010-12, ($/W)

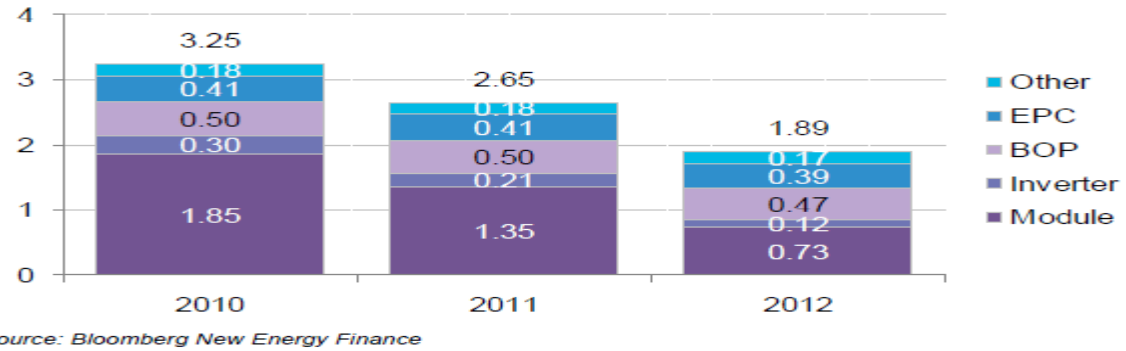

Source: Bloomberg New Energy Finance

Appendix V

Hydro Price

Hydro

For this report we split hydro into two categories: large dams over 10MW and small dams under 10MW, which includes run-of-river projects. The WEC Survey of Energy Resources published in 2013 indicates that there is a substantial potential for further development of small hydro and run-of-river capacity as well as for large hydro. While hydropower has already been exploited to a high degree in Europe (75%) and North America (69%), there still is significant potential in Latin America (33%), Asia (22%) and particularly in Africa (7%).

Table 13

Levelised cost of hydro electricity globally

Source: Bloomberg New Energy Finance.
Note: *the given range is an average scenario and does not reflect actual maximum and minimum values

Geography	CAPEX (USDm/MW)	OPEX (USD/MW/yr)	Capacity factor (%)	LCOE (USD/MWh)
Small hydro	1.40–3.68	15,002–85,000	23–80	19–314
Large hydro	1.59–4.15	20,000–62,000	20–75	24–302

CAPEX- Capital Expenditure- money invested by a company.

Appendix VI

Project site's population and facility data from the Wereda administration office.